

*Advanced Magnetic Flux Compression
Generator Development Issues: A Comparison
of Coaxial and Disk Generators*

Maurice G. Sheppard

Bruce L. Freeman



ADVANCED MAGNETIC FLUX COMPRESSION GENERATOR DEVELOPMENT ISSUES: A COMPARISON OF COAXIAL AND DISK GENERATORS

by

Maurice G. Sheppard and Bruce L. Freeman

ABSTRACT

Three magnetic flux compression generator (FCG) geometries are reviewed and compared for their suitability as high-current, high-power drivers for z-pinch implosion programs at Los Alamos. They are the inside-out coaxial FCG, the disk FCG, and the outside-in coaxial FCG. A wide range of issues is discussed for each type FCG including current-carrying capability, current densities, robustness, explosive mass and shape, initiation schemes, efficiency, operating times, complexity, and expense associated with development and fabrication. Equations are derived and used in simple scaling studies. The results of these studies are supported by MHD calculations and references to relevant experiments both here and in Russia. The inside-out coaxial FCG is shown to be suitable, both for the very high current applications and for anticipated future Trailmaster concepts. Based upon this analysis and results reported in the Russian literature, the inside-out coaxial FCG is more suitable than the disk FCG for the high-current applications considered, and the two are roughly equivalent when applied to lower-current Trailmaster concepts. The outside-in coaxial FCG is unsuitable for either application because of its limited current-carrying capability and the large investment required for initial development.

I. INTRODUCTION

This report is an attempt to review objectively the salient features of three different geometries for explosive flux compression generators (FCG). In particular, these FCGs are compared as possible final stage pulsed power drivers for z-pinch liner implosions. Figures 1, 2, and 3 show schematic drawings of an inside-out coaxial FCG, a disk FCG, and an outside-in coaxial FCG, respectively. An attached imploding liner is also shown with its required

DISK FCG

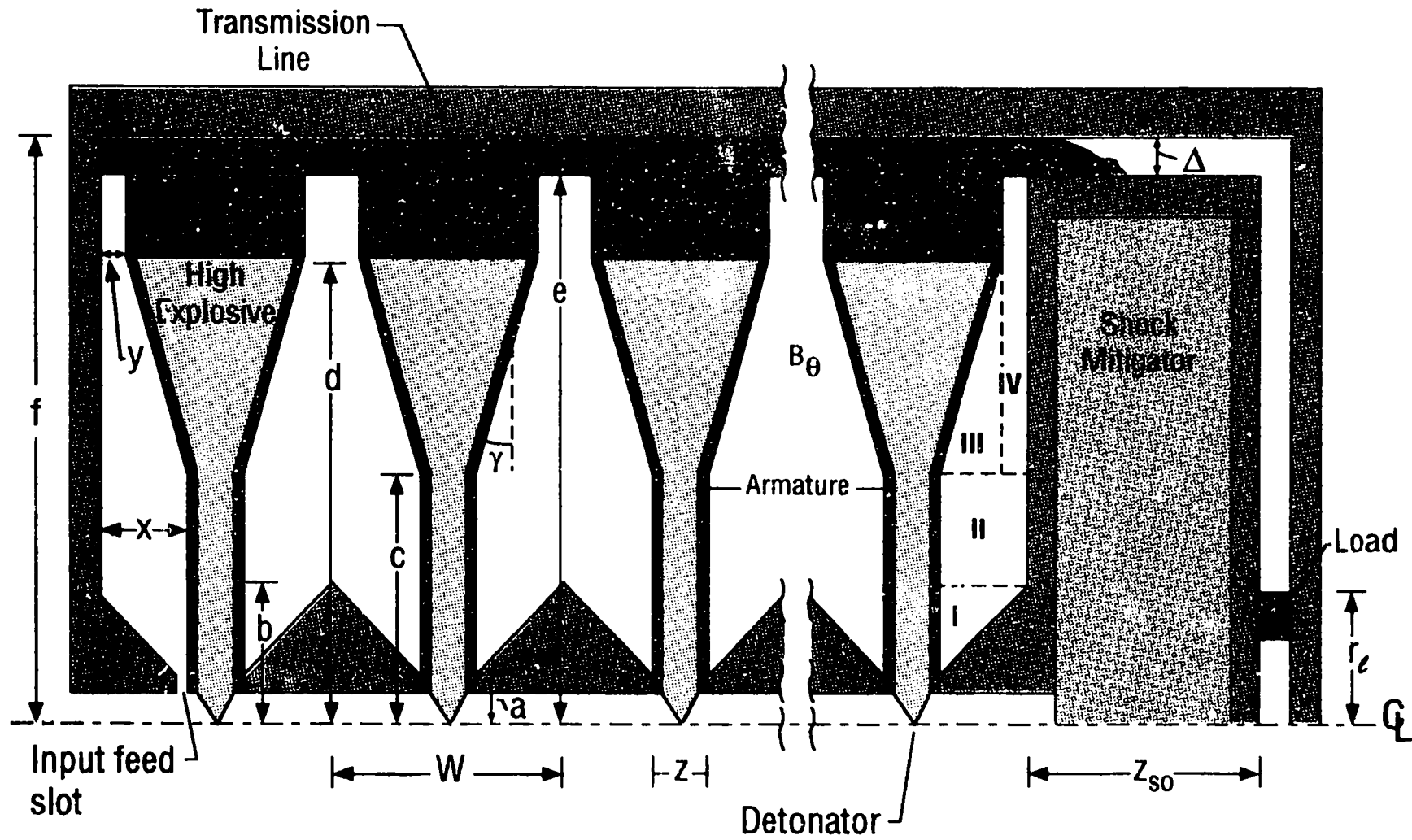


Fig. 1. Generic inside-out simultaneous coaxial FCG.

INSIDE-OUT SIMULTANEOUS COAXIAL FCG

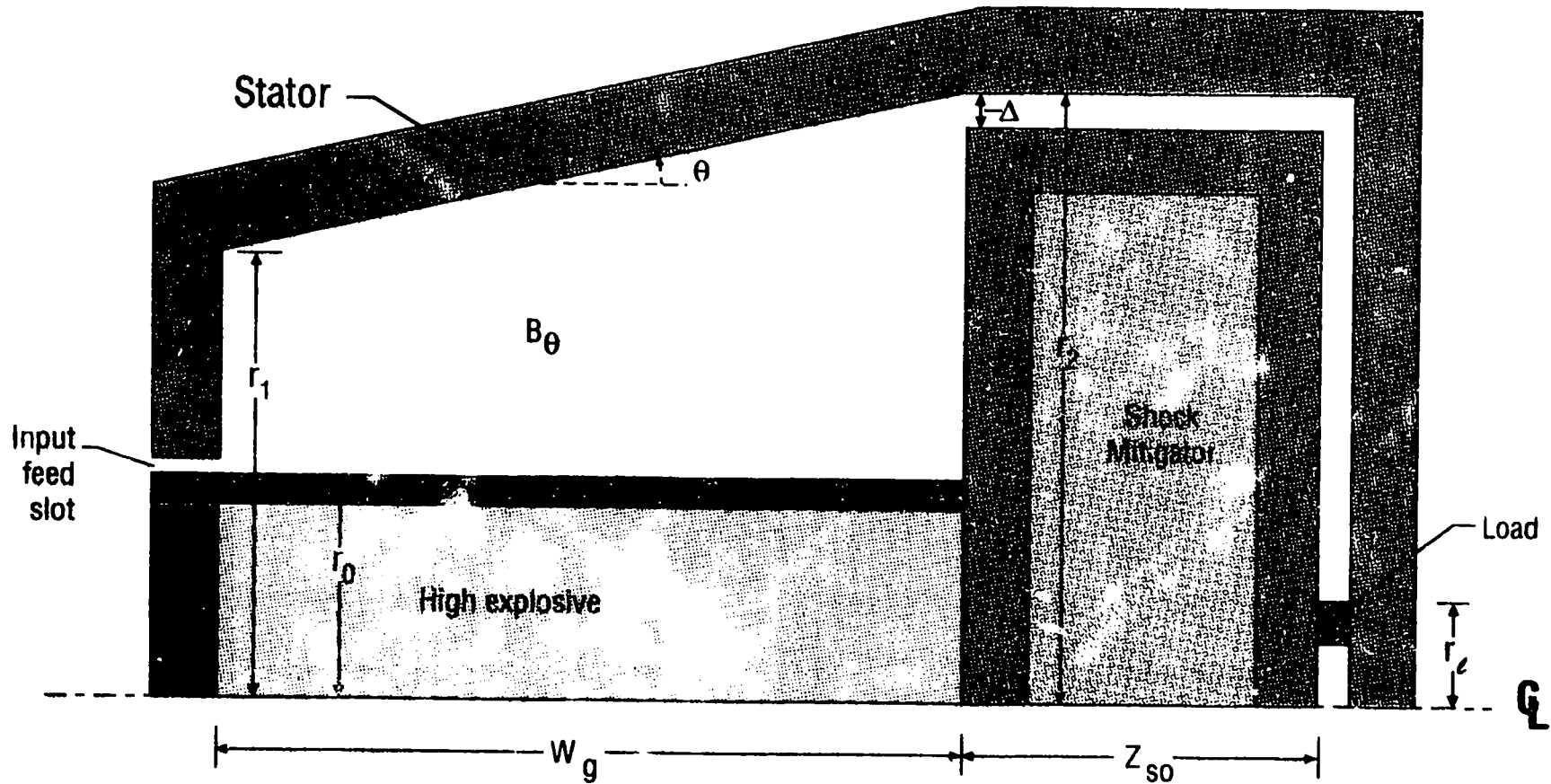


Fig. 2. Generic disk FCG.

OUTSIDE-IN SIMULTANEOUS COAXIAL FCG

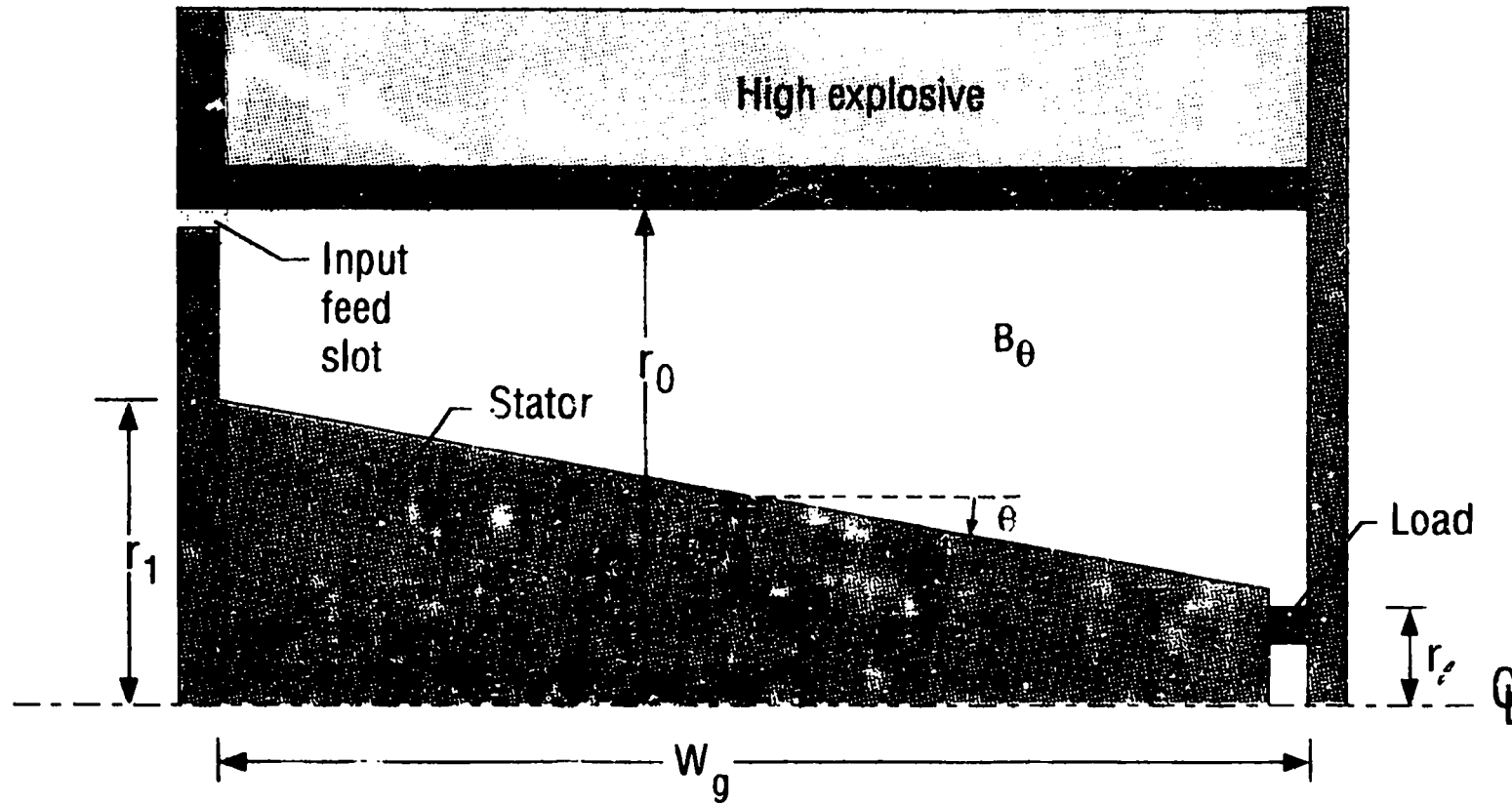


Fig. 3. Generic outside-in simultaneous coaxial FCG.

transmission line. The discussions are not exhaustive, and many of the qualitative predictions (particularly for the disk and outside-in coaxial FCGs) have not been verified by experiments in this country. The discussions of the inside-out coaxial FCG require the use of existing hardware, such as the HE system, so hypothetical performance is balanced by LANL capability. For the disk FCGs, data from Russian reports are used, where available. In the absence of such information, optimistic assumptions are used. Enough detail has been provided so that the interested reader may reproduce the analysis with different parameters and further investigate the sensitivity of the results to the assumptions concerning FCG performance.

The primary pulsed power requirements for the purposes of this discussion are currents of 150 MA delivered with a final risetime of $\sim 10 \mu\text{s}$ into a low-inductance, closely coupled imploding load. Some consideration will also be given to lower currents ($\sim 50 \text{ MA}$) delivered in shorter times into higher inductance loads, specifically relevant for the Trailmaster program. Some of the issues to be discussed include (1) linear current density on the armature, both for the initial loading current and the final peak current, (2) magnetic field energy density or pressure, $B^2/(2\mu_0)$, (3) armature travel distance, (4) transmission-line inductance and stand-off distance for load protection, (5) cost, flexibility, and availability of high-explosive (HE) initiation systems for each geometry, (6) HE mass, shape, and efficiency of use, (7) operation time of the FCG, (8) ideal current amplification and expected efficiencies for flux loss, (9) seed-field energy requirements, (10) fabrication and assembly difficulties and complexities, and (11) environmental considerations.

The next section discusses general considerations associated with generating fast, high-current pulses. Each generator type is discussed in more detail in the following three sections. Supporting calculations and references are given where available. For purposes of comparison, a 5-cm-radius, 1-cm-wide cylindrical shell is chosen as the active load. To make the analysis simpler and more transparent, it is assumed that the current risetime is fast enough and that the imploding load is massive enough so that significant displacement of the load does not occur before peak current and generator burnout. Resistive losses in the load are also assumed to be small compared to losses in the FCG. None of these assumptions is crucial or difficult to remove; therefore, the qualitative conclusions are not compromised by the simplification. These assumptions are equivalent to specifying a purely static inductive load. Following the specific discussions of each generator type, a comparison of disk and coaxial FCG drivers is presented for powering larger inductive loads that require lower currents. The final section summarizes the findings and attempts to draw conclusions that point the way towards future advanced generator development.

II. GENERALITIES

A. High Currents

The generation of high currents (≥ 50 MA) requires large area conductors in order to keep linear current densities to a reasonable value. A well-known rule of thumb among FCG designers is that the armature should not carry more than $J_z \approx 1$ MA/cm during its entire operation.¹ In coaxial geometry with axial currents and only azimuthal magnetic fields, a total current of 150 MA requires a conductor radius of at least 24 cm in order to keep $J_z < 1$ MA/cm. Given $B_\theta = \mu_0 I / (2\pi r) = \mu_0 J_z$, the magnetic field associated with $J_z = 1$ MA/cm is $B_\theta = 1.26$ MG, and the magnetic field energy density and associated pressure, $B_\theta^2 / (2\mu_0)$, are 6.3 GJ/m³ and 63 kbar, respectively. To put these numbers in perspective, the energies required to melt Al and Cu are approximately 0.15 and 0.32 GJ/m³, respectively, and their yield strengths are only about 2–3 kbar. Using the HE, PBX-9501, to push the armature will initially drive a ~ 300 -kbar shock through the armature. However, the sustained pushing pressure drops quickly to less than 50 kbar as the armature begins to move and the HE thermalizes into a hot expanding gas. In other words, as the magnetic field reaches ~ 1 MG during flux compression, the armature kinetic energy, driven by the HE gases, is overpowered by the opposing magnetic back pressure, and/or the current-carrying side of the armature is vaporized by resistive heating, limiting its ability to continue to compress magnetic flux.

The use of helical generators, such as the Mark IX,² to generate greater than 50 MA is limited by the 1-MA/cm limit because the number of bifurcations in the stator windings that would be required to get enough parallel wires to carry the current rapidly becomes prohibitive at high current. Magnetic pressures present at the stator can also cause undesired motion of the windings.

The 1-MA/cm limit has been more or less confirmed in Russian experiments with large disk FCGs. Both Pavloskii^{1,3} and Chernyshev^{4–7} have fielded disk FCGs, which push but do not exceed this limit, and they indicate that higher currents can be achieved only by accepting larger radius generators. At Los Alamos, the CN-III high-current coaxial FCG also challenged and confirmed this limit in its last experiment.⁸ The first experiment was an armature case motion study without magnetic fields. The second was a low current shot with a 1-MA seed current and a final current of 68 MA. The third experiment started with a 3-MA seed current and produced a peak current of 105 MA. This measurement corresponds to a linear current density of ~ 0.7 MA/cm on the armature at peak current. For the last CN-III experiment, the initial radius of the armature was increased, and the propagation section of HE was replaced with a simultaneous section. This allowed more HE inside the armature, reduced the armature travel distance, and reduced generator operating time. The

stator radius at the entrance to the load ring for the CN-III is 27.5 cm. The final current for the fourth CN-III experiment was above 150 MA and produced almost 1 MA/cm on the armature. All CN-III experiments were extensively modeled with the RAVEN code. RAVEN is a sophisticated one-dimensional Lagrangian MHD code written by Tom Oliphant and used extensively in the Los Alamos National Laboratory's group X-5.⁹ In RAVEN's quasi-2D mode, multiple 1D-MHD calculations are run simultaneously and coupled through a sophisticated circuit package. Each 1D calculation, referred to as a module, represents a different axial section of the FCG. The sum of all modules, running simultaneously and coupled, reflects the most important 2D characteristics of the FCG. Similar modules can be run in a vectorized mode.

A relaxation of the 1-MA/cm rule-of-thumb limit would permit additional flexibility in FCG design. Both the magnetic back pressure and the resistive Joule heating of the conductors require time before their effect is significant. Therefore, significantly faster generators may be capable of exceeding the 1-MA/cm limit. There are several ways to decrease the run time of an FCG. Increasing the armature velocity and/or using explosive to push both the armature and the stator as in the 1×4 plate generator, are two options. Higher velocities can be achieved by using lower density and/or thinner armatures. However, fundamental limitations are imposed by HE energy density, armature integrity, and armature current carrying capability. Reasonable armature velocities (v_{arm}) for copper and aluminum, driven by PBX-9501, range from 0.1 to 0.4 cm/ μ s. Another option for speeding up the FCG is to reduce the armature/stator separation. Unfortunately, a penalty in FCG inductance is incurred when exercising this option.

Convergence effects have been used in imploding liner experiments to produce greater than 6 MG in very small volumes.¹⁰ The 1-MA/cm criterion is obviously exceeded in these experiments but not in a geometry or on a timescale, which is useful for a FCG that must power an external load.

B. Fast Risetimes

The fast operating times required by the specific applications considered here add another level of complexity. For the inside-out and the outside-in coaxial FCGs, the most effective way to shorten the operation time is to simultaneously initiate the explosive along the entire length of the armature. Given an HE detonation velocity (v_{det}) of 0.88 cm/ μ s, the operation time of an 88-cm-long coaxial FCG can be reduced by 100 μ s if the HE is initiated simultaneously rather than detonated at one end in the traditional fashion. Two systems exist for this purpose and have been used for simultaneous inside-out FCGs. The first is a line initiation system consisting of evenly-spaced slapper detonators on axis. This system has been successfully used in the CN-I, CN-II,¹¹ and the Mark 101^{12,13} FCGs as well

as in the explosively formed fuse (cutter switch) used in the Trailmaster experiments. The other possibility is the Falcon tile system, which has been used successfully in the CN-III experiments.⁸

Operating times for coaxial FCGs are also affected by armature travel distance and armature velocity. Reducing the armature/stator separation speeds up operation at the expense of FCG inductance. Additional inductance may be obtained by lengthening the FCG. However, a reasonable limit of ~ 3 m may be imposed by material handling and availability as well as HE volumes and mechanical assembly. Armature velocities are affected by the amount and type of explosive used and by the armature thickness and density.

Operation time for a disk FCG is basically controlled by the burn time of the explosive, which is detonated on axis and burns radially. The armature travel distance is quite small at larger radii (~ 1 cm in Russian designs)^{1,3-7} and does not contribute significantly to the operating time. The disk FCG makes use of opposing armatures in the same way as the 1×4 plate FCG. Therefore, a 30-cm radius disk FCG, loaded with PBX-9501 has a total operating time of $\sim 35 \mu\text{s}$, not counting the initial seed field loading time.

C. Low Inductance Loads

There are two related reasons for desiring low inductance loads when very high currents need to be produced. First, the current amplification factor for an FCG is proportional to the ratio of initial FCG plus load inductance to final load inductance. For purposes of calculating current amplification, the inductance of the transmission line, which connects individual modules of a disk FCG, must be included as part of the load inductance. A larger load inductance requires either a larger generator inductance or a higher initial seed current to reach the same final current. Both of these options add to the expense. The related factor is that every nanohenry of load inductance must be filled with magnetic field energy. At a load current of 150 MA, extra load inductance costs energy at the rate of 11.2 MJ/nH.

Load inductance is controlled by several variables including: (1) required standoff distance from the HE charge, (2) radius of the power-flow channel where it connects to the FCG, and (3) inductance left in the FCG at burnout. For the inside-out coaxial FCG and the disk FCGs, the standoff distance and the radius of the power flow channel are fixed by the generator operating time and the maximum current, respectively. For a 1-cm-wide channel with an outer radius of 30 cm, each 15 cm of standoff adds an extra 1.02 nH to the load inductance. An inside-out coaxial FCG requires a larger standoff distance than a disk FCG of the same radius because the required armature/stator separation distance at the output end of the coaxial FCG results in a longer run time. However, a disk FCG of 30-cm radius with a 1-cm-wide transmission line connecting the modules would leave 1.02-nH worth of inaccessible inductance for every 15 cm of generator length. This waste inductance estimate

is based upon high-current Russian designs, which all appear to have a 1-cm-wide, dielectric-filled channel connecting each disk module.^{1,3-5} Lower current disks have narrower channels and smaller radii.^{6,7}

The outside-in coaxial FCG appears to have a significant advantage with respect to load inductance. No standoff distance is required and, at first glance, no waste inductance is left in the generator at burnout. However, if the inner stator has a radius of $r_2 = 5$ cm, the armature would have to be imploded all the way to 5 cm in order to completely wipe out all of the generator inductance. At 150 MA, this diameter implies a linear current density of 4.8 MA/cm on the armature, significantly violating the accepted rule of thumb discussed earlier. As shown in a later section, RAVEN calculations predict that the outside-in coaxial FCG with a stator at 5-cm radius would fail before reaching the required 150 MA.

III. INSIDE-OUT SIMULTANEOUS COAXIAL FCG

The inductance of the load and transmission line assembly shown in Fig. 1 is given by

$$L_l(nH) = \mu_o [z_{so} \cdot \ln(r_2/(r_2 - \Delta)) + w \cdot \ln(r_2/r_l)] / (2\pi) \quad , \quad (1)$$

where z_{so} is the required standoff distance, r_2 is the outside radius of the transmission line (and the inside radius of the stator), r_l is the load radius, w is the width or separation between the vertical load walls, which is taken to be 1 cm throughout, and Δ is the transmission line thickness. The generic FCG is also shown in Fig. 1 where r_o , r_l , and r_2 define the armature and stator radii, W_g is the generator length and θ is the tilt angle of the stator required for phased flux compression.

Using experience gained from the CN-III high-current FCG experiments and calculations,⁸ the following assumptions are used in this scaling study. First, to conservatively generate 150 MA reliably and reproducibly, requires a stator radius of $r_2 = 30$ cm, giving $J_x^{\max} = 0.8$ MA/cm at FCG burnout. Experience with CN-II,¹⁰ CN-III,⁸ and other FCG's,^{12,13} imposes a conservative limit on armature expansion. To be safe, an armature tube should be expanded no more than a factor of two times its initial radius. The smallest stator radius allowed by this constraint is $r_o = r_2/2 = 15$ cm. A stator tilt angle of 2.5° and a maximum reasonable length of $W_g = 300$ cm fixes $r_l = r_2 - W_g \cdot \tan \Theta = 16.9$ cm. Generator inductance (L_g) is given by

$$L_g = \mu_o W_g [\ln(r_l/r_o) + r_2 \cdot \ln(r_2/r_l) / (r_2 - r_l) - 1] / (2\pi) \quad , \quad (2)$$

which gives $L_g = 260$ nH for this specific example. Operation time of the FCG is estimated by assuming that the armature tube is filled with PBX-9501, which has a detonation velocity

of $v_{\text{det}} = 0.88 \text{ cm}/\mu\text{s}$ and pushes a 1-cm-thick aluminum armature with a velocity of $v_{\text{arm}} = 0.23 \text{ cm}/\mu\text{s}$. Operation time from first armature motion through burnout is obtained from

$$t_{op} = (r_2 - r_o)/v_{\text{arm}} \quad , \quad (3)$$

which gives a value of $65.22 \mu\text{s}$ for this example. Adding the time required for the HE detonation wave to propagate from the axis and begin moving the armature gives a standoff time,

$$t_{so} = r_o/v_{\text{det}} + t_{op} \quad (4)$$

of $85 \mu\text{s}$. Given a sound speed of $0.2 \text{ cm}/\mu\text{s}$ in lead and in polyethylene, it is reasonable to assume that layers of lead, polyethylene, and air could be designed that would mitigate shocks at a standoff distance of

$$z_{so} = v_{so}t_{so} \quad (5)$$

for a time of t_{so} , where $v_{so} = 0.2 \text{ cm}/\mu\text{s}$. In this example the standoff must be 16.5 cm , which implies a load inductance of $L_l = 4.7 \text{ nH}$ if $\Delta = 1 \text{ cm}$.

Ideal current amplification of an L_g inductance FCG driving an L_l inductance load is

$$(I_f/I_o)_{\text{ideal}} = (L_g + L_l)/L_l \quad . \quad (6)$$

Based upon CN-III experience, one can expect an actual current amplification that is 70% of ideal. Using this assumption, Eq. (6) gives a realistic current amplification factor of 39.4. An initial current of $I_o = 3.8 \text{ MA}$ would then be sufficient to produce a final current of $I_f = 150 \text{ MA}$. This initial current corresponds to an initial seed field energy of

$$E_o = (L_g + L_l)I_o^2/2 = 1.9 \text{ MJ} \quad , \quad (7)$$

and a final field energy in the load of

$$E_f = L_l I_f^2/2 = 52.9 \text{ MJ} \quad . \quad (8)$$

The mass of HE contained in the FCG is

$$M_{\text{HE}} = \rho\pi W_g (r_o - t)^2 = 3.4 \times 10^5 \text{ g} \quad , \quad (9)$$

which is equivalent to 750 lbs. Here we have assumed a 1-cm-thick armature ($t = 1 \text{ cm}$) and that the HE fills the entire central volume. At an energy density of 5.5 kJ/g for PBX-9501, this HE mass corresponds to 1870 MJ of chemical energy, of which 2.7% is converted to magnetic field energy. Demonstrated efficiencies for FCGs range from 1 to 10%.^{14,15}

The foregoing analysis is summarized in Table I along with similar analyses for a 150-cm-long FCG and one that has a 200-cm-long, 20-cm-radius armature. The latter FCG would operate on a shorter timescale because of the reduced armature travel distance, but have less inductance per unit length. The last column in the table shows an FCG design, which should be capable of generating a 250-MA pulse, albeit with a longer risetime caused by the increased armature/stator separation. Unfortunately, the operating time for any of these FCGs is longer than 10 μ s. A detailed analysis will be required to quantify the risetime requirement.

Table I. Sample inside-out coaxial FCGs.

Property	1	2	3	4
W_g (cm)	300	150	200	300
r_o (cm)	15	15	20	25
r_1 (cm)	16.90	23.45	26.51	36.90
r_2 (cm)	30	30	30	50
θ	2.5°	2.5°	1.0°	2.5°
t_{op} (μ s) ^a	65.22	65.22	43.48	108.70
t_{so} (μ s) ^{a,b}	82.26	82.26	66.21	137.10
z_{so} (cm) ^c	16.45	16.45	13.24	27.42
Δ (cm)	1.0	1.0	0.5	1.0
L_g (nH)	260.1	172.5	138.0	329.4
L_l (nH)	4.70	4.70	4.03	5.71
$0.70 \cdot (I_f/I_o)_{ideal}$	39.45	26.40	24.67	41.06
I_o (MA)	3.80	5.68	6.08	6.09
E_o (MJ)	1.91	2.86	2.62	6.21
I_f (MA)	150	150	150	250
E_f (MJ)	52.86	52.86	45.32	178.5
M_{HE} (kg) ^d	340	170	417	1000
W_{HE} (lbs) ^d	748	374	918	2200
E_{HE} (MJ) ^d	1870	935	2300	5500
J_x^o (MA/cm)	0.04	0.06	0.05	0.04
$(E_f - E_o)/E_{HE}$	2.73%	5.35%	1.86%	3.14%

^a Assumes $v_{arm} = 0.23$ cm/ μ s.

^b Assumes $v_{det} = 0.88$ cm/ μ s.

^c Assumes $v_{so} = 0.20$ cm/ μ s.

^d Assumes a 1-cm-thick Al armature and PBX-9501.

One complication that arises when going to larger diameter charges of HE is the pressing and machining limits imposed by hardware and safety considerations at WX-3. The largest radius charge of PBX-9501 that can be pressed and machined at Los Alamos is ~ 23 cm. In addition, the number of HE glue joints required during assembly (because standard operating procedures dictate an HE single-piece, machining weight limit of 70 lbs) becomes oppressive

as the length of the armature approaches 300 cm. The obvious solution to these problems is the development of a high-energy-density castable explosive. Not only would this capability dramatically increase the design flexibility for inside-out coaxial FCGs, but it is an absolute necessity for affordable outside-in designs and disk generators. A castable explosive should also be cheaper in the long run since costs associated with precision gluing and machining of HE parts would be eliminated.

IV. DISK FCG

Figure 2 illustrates a generic disk FCG with its attached load, where the only difference between the load for a disk and an inside-out coaxial FCG is the required standoff distance. Like the coaxial FCG, only the azimuthal component of the magnetic field, B_θ , is non-zero for the disk FCG. From an electromagnetic point of view, the disk armature is isomorphically a coaxial armature that has been fluted or folded, like an accordion.

The inductance calculation for the disk is divided into the four regions shown in Fig. 2, and the results are tabulated below. The inductance per module is given by

$$L_g = 2(L_I + L_{II} + L_{III} + L_{IV}) \quad , \quad (10)$$

where

$$L_I = \mu_o x (1 + a \cdot \ln(a/b)/(b-a))/(2\pi) \quad , \quad (11)$$

$$L_{II} = \mu_o x \cdot \ln(c/b)/(2\pi) \quad , \quad (12)$$

$$L_{III} = \mu_o (x - y) (d \cdot \ln(d/c)/(d-c) - 1)/(2\pi) \quad , \quad (13)$$

and

$$L_{IV} = \mu_o y \cdot \ln(e/c)/(2\pi) \quad . \quad (14)$$

It is assumed that the HE wipes out 100% of L_g but leaves the connecting transmission line between radii e and f uncompressed. In high-current Russian generators, this transmission line is dielectric-filled and appears to be 1-cm wide. The inductance associated with the transmission line is given by

$$L_t = \mu_o W \cdot \ln(f/e)/(2\pi) \quad , \quad (15)$$

where W is the width of a single module. There is one constraint associated with the choice of parameters c and x , which is related to the detonation velocity and the armature velocity. The angle g , shown in Fig. 2, must be less than

$$\gamma_{\max} = \sin^{-1}(v_{\text{arm}}/v_{\text{det}}) \quad (16)$$

to insure proper phasing of the flux compression. A larger angle than γ_{\max} would cause the output to close off before all flux is transferred from the generator to the transmission line and load. In this study, γ is chosen to be $\gamma_{\max} - 1^\circ$ for the 30-cm-radius disk FCG. This choice gives a 2° closure angle during flux compression. For very high current operation with minimum explosive mass, the magnetic back pressure during flux compression can affect the choice of γ . This concern should be investigated with two-dimensional MHD calculations for actual FCG designs.

As in the description of the coaxial FCG in the previous section, a specific example for a disk FCG is worked out in detail below. A conservatively designed disk FCG capable of producing 150 MA into the given load might have the dimensions 5, 10, 10.15, 28, 29, and 30 cm for the radii a , b , c , d , e , and f , respectively (see Fig. 2). As in the design for the coaxial FCG of the previous section, the maximum linear current density at 30 cm would only be 0.8 MA/cm. Setting x , y , and z to 5, 0.5, and 5 cm gives a width per module, $W = 2x + z$, of 15 cm. Using Eqs. (10)–(14) gives an inductance, L_g , of 19.19 nH per module with a transmission line inductance, L_t , given by Eq. (15), of 1.02 nH per module.

Operating time for the disk is given approximately by

$$t_{op} = (d - a)/v_{det} + y/v_{arm} \quad , \quad (17)$$

whereas the standoff time for load protection is computed from

$$t_{so} = a/v_{det} + t_{op} \quad . \quad (18)$$

Using parameters for PBX-9501 again, and assuming that a 0.5-cm-thick copper armature could be pushed at $v_{arm} = 0.23$ cm/ μ s, gives $t_{op} = 28.31$ μ s and $t_{so} = 33.99$ cm/ μ s. Equation (9) gives 6.80 cm for z_{so} and results in a load inductance L_l of 4.04 nH.

The mass of explosive per module is calculated from

$$M_{HE} = \pi(z - 2t)d^2 + 2\pi(x - y - t)(2d^2 - dc - c^2)/3 \quad , \quad (19)$$

where t is the thickness of the armature. Reductions in HE mass are possible by including inert wedges near the outer radius. For the case being studied, there are 36.33 kg (or 79.92 lbs) of HE per module. This explosive mass amounts to 200 MJ of chemical energy per module. A disk of N_d modules would have a total inductance $L_G = N_d L_g$ and an effective load inductance $L_L = N_d L_t + L_l$. The ideal current amplification for such a generator is given by

$$(I_f/I_o)_{ideal} = (L_G + L_L)/L_L \quad . \quad (20)$$

From the Russian literature, it is not unreasonable to expect an actual amplification that is 75% of ideal.^{1,3-7} As an example, a 300-cm disk assembly of $N_d = 20$ modules, would

have an inductance of 384 nH, a load inductance of 24.4 nH, and an actual current amplification of 12.6. To achieve 150-MA output would require 12.0-MA input seed current, which corresponds to 29.3 MJ of input seed field energy and an output field energy of 274 MJ. The HE mass in a 20-module disk would be 727 kg (1600 lbs), which means 6.1% of the total 4000 MJ of chemical energy must be converted to electromagnetic energy. The linear current density at radius $a = 5$ cm during the loading of a disk generator to 12.0 MA is 0.38 MA/cm. At 0.38 MA/cm there will be some motion of the armature during loading. Decreasing the preliminary loading time through clever switching would ameliorate the undesired armature motion. Table II summarizes these estimates and includes scaling for a 10-module disk. It also gives parameters for a more optimistic 30-cm-radius disk, which has a 0.5-cm-thick transmission line. The most critical design parameter affecting disk performance in an energy-constrained regime is the 1.02 nH per module of waste inductance. By cutting the transmission line gap in half, L_t becomes 0.50 nH. However, this small gap reduces the overall robustness of the design. Cutting the insulation gap even further to 0.25 cm (100 mil), would only reduce the transmission line inductance to 0.25 nH per module, or 5 nH for a 20-module, 30-cm-radius disk. Holding off internal FCG voltages — which may easily exceed 100 kV at these current and power levels — in the presence of HE-driven shocks, would be a challenge. Nevertheless, enough detail has been provided for the ambitious reader to explore extrapolated FCG performance in these regimes. Finally, Table II gives parameters for a disk FCG that should be capable of producing 250 MA. The parameters come almost directly from a paper by Chernyshev in which he reports 256 MA into a 3.3-nH load, including the connecting transmission line, using a 3-module disk FCG.⁵

Disk FCGs have both favorable and unfavorable characteristics as drivers for the load being considered. In favor of the disk is the fact that operating times are somewhat shorter and armature travel distance is shorter than for the equivalent coaxial FCG. For these reasons, a disk FCG will more likely be able to exceed the 1-MA/cm limit than a coaxial device. Unfortunately, neither type is likely to exceed the limit by much, given HE performance figures. The disk also has the advantage that the initiation system is simpler and requires only N_d simultaneous detonators on axis, whereas the coaxial system needs either a line or area initiator. Finally, the fact that the Russians have reported a 256-MA peak current from a 3-module, 50-cm-radius disk is noteworthy. On the negative side, disk FCGs have multiple complicated HE shapes. Pressing and machining 30-cm-radius disks of HE is not cost-effective, given the complex shapes required. Castable and liquid explosives exist, but not at the energy density of PBX-9501. Assembly for the disk is also likely to be a challenge. It has many pieces and many potentially troublesome and lossy conductor joints perpendicular to the direction of

current flow. Because the HE charge extends to large radius, disk FCGs will have relatively large amounts of explosive. However, this extra explosive is strategically concentrated near the output feed slots where the magnetic field will be the highest.

Table II. Sample disk FCGs.

Property	1	2	3	4
a (cm)	5	5	5	6
b (cm)	10	10	10	12
c (cm)	10.15	10.15	10.65	24
d (cm)	28	28	28.50	48
e (cm)	29	29	29.50	49
f (cm)	30	30	30	50
$\Delta = f - e$ (cm)	1.0	1.0	0.5	1.0
x (cm)	5	5	5	5
y (cm)	0.5	0.5	0.5	0.5
z (cm)	5	5	5	5
$W = 2x + z$ (cm)	15	15	15	15
L_g (nH)	19.19	19.19	19.72	28.38
L_z (nH)	1.02	1.02	0.50	0.61
L_t (nH)	4.04	4.04	3.82	5.06
t_{op} (μ s) ^a	28.31	28.31	28.88	49.90
t_{so} (μ s) ^a	33.99	33.99	34.56	56.72
z_{so} (cm) ^b	6.80	6.80	6.91	11.34
N_d	20	10	13	20
$W_G = N_d \cdot W$ (cm)	300	150	195	300
$L_G = N_d \cdot L_g$ (nH)	383.7	191.9	256.4	567.6
$L_L = N_d \cdot L_t + L_l$ (nH)	24.39	14.21	10.37	17.19
$0.75 \cdot (I_f/I_o)_{ideal}$	12.55	10.87	19.29	25.52
I_o (MA)	11.95	13.80	7.77	9.80
E_o (MJ)	29.14	19.61	8.06	28.06
I_f (MA)	150	150	150	250
E_f (MJ)	274.3	159.9	116.7	537
$N_d \cdot M_{HE}$ (kg) ^c	727	363	486	2000
$N_d \cdot W_{HE}$ (lbs) ^c	1600	799	1070	4300
$N_d \cdot E_{HE}$ (MJ) ^c	4000	2000	2670	10700
J_x^o (MA/cm)	0.38	0.44	0.25	0.26
$(E_f - E_o)/E_{HE}$	6.14%	7.02%	4.06%	4.74%

^a Assumes $v_{arm} = 0.23$ cm/ μ s and $v_{det} = 0.88$ cm/ μ s.

^b Assumes $v_{so} = 0.20$ cm/ μ s.

^c Assumes a 0.5-cm-thick Cu armature and PBX-9501.

V. DIRECT COMPARISON BETWEEN DISK FCG'S AND INSIDE-OUT COAXIAL FCG'S

Figures 4–30 provide a direct comparison between inside out coaxial FCGs and disk FCGs. The basis for the comparisons are the examples used in the previous two sections. The first set of graphs compares, as a function of length, a family of 30-cm-radius disk FCGs, capable of producing 150 MA into the generic load and transmission line, against a continuum of coaxial FCGs of the same radius and peak current. The conservative parameters from column 1 of Tables I and II are used to define the geometries for the coaxial and disk FCGs, respectively. Figure 4 gives the FCG inductance, which is linear with W_g for the disk and only defined at integral multiples of the unit module length, $W = 15$ cm. The inductance for the coaxial FCG falls below linear because of the required tilt angle of the stator. The effective load inductance for the two FCG families is shown in Fig. 5. The linear rise for the disk is a direct result of the unusable transmission line inductance associated with each module. Figure 7 shows the expected current gain for the two FCGs using 70% of ideal for the coaxial and 75% for the disk. Using the results of Figs. 4 and 6, Figs. 7 and 8 give the required initial current and magnetic field energy, which must be loaded into the FCGs to insure 150 MA of output current. The larger inductance per unit length coupled with the lower current gain of the disks relative to the coaxial FCGs, results in substantially larger initial loading energies. The final magnetic field energy, which is stored into the effective load inductance at 150 MA, is given in Fig. 9. High-explosive weight is shown in Fig. 10, and Fig. 11 gives the required efficiency of conversion from chemical to magnetic field energy. For reference, the total HE capacity at Firing Point 88 in Ancho Canyon is 2000 lbs. Interpretation of Fig. 11 is tricky because a higher required efficiency is more difficult to achieve. Anything above ~10% efficiency is speculative. Within each type, the robustness of the generator is inversely related to its required efficiency. Inserting inert wedges into the disk charges, while decreasing the overall HF weight, increases the required efficiency of the FCG, and introduces additional complexity in the assembly and charge configuration. The final graph for this first set of comparisons, Fig. 12, is the maximum linear current density, which must be sustained during the initial loading. Current densities required for the disk are high enough to cause concern about magnetically induced motion of the armature during the loading process prior to HE-supported motion. In choosing an optimal length for either of the FCGs, the information in Figs. 4–12 needs to be considered as a whole in conjunction with expense, the availability of initial current sources, and reasonable firing point facility capacity.

Using parameters from Table II for the more optimistic disk FCG, with a 0.5-cm transmission line gap, and comparing it to an optimistic coaxial FCG with a faster operation time, gives the comparison presented in Figs. 13–21. For the coaxial FCG the armature tilt angle,

θ , is reduced to 1° ; Δ is reduced to 0.5 cm to match the transmission line in the disk; and r_o , the armature radius, is increased to 20 cm. The increase in r_o decreases the operating time from 65.22 μs for the coaxial in the first comparison, to 43.48 μs . The operating time of the disk increases by only 0.57 μs to 28.88 μs .

The final set of graphical comparisons is given in Figs. 22-30 for the 250-MA cases presented in Tables I and II. In all cases considered, an inside-out FCG is expected to exceed the performance of the equivalent disk FCG for this high-current application. As mentioned earlier, the biggest drawback of the disk FCG is wasted inductance in the required transmission line, a by-product of its modularity. This inductance hurts current amplification, which in turn requires larger seed currents. Larger seed currents are expensive and potentially cause problems associated with conductor deformation prior to HE-supported motion. The extra inductance must be filled with the same magnetic field energy per nanohenry as the load. The larger output energy requires higher efficiencies from the disk, probably making it less robust. The extent to which this inductance can be minimized is a topic for research and will depend upon such variables as required voltages, breakdown fields in shocked dielectrics, shock mitigation in the dielectric channel, and magnetic insulation.

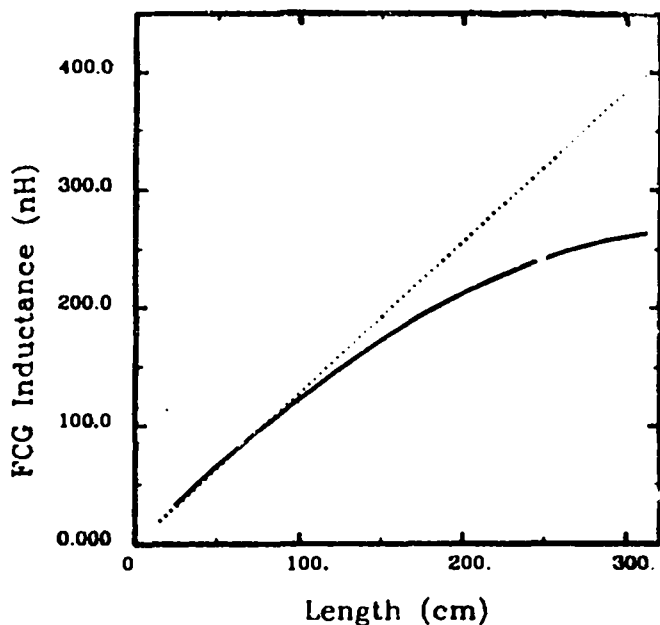


Fig. 4. Inductance vs length for 30-cm-radius inside-out coax (solid) and disk (dotted) FCGs with $\Delta = 1$ cm.

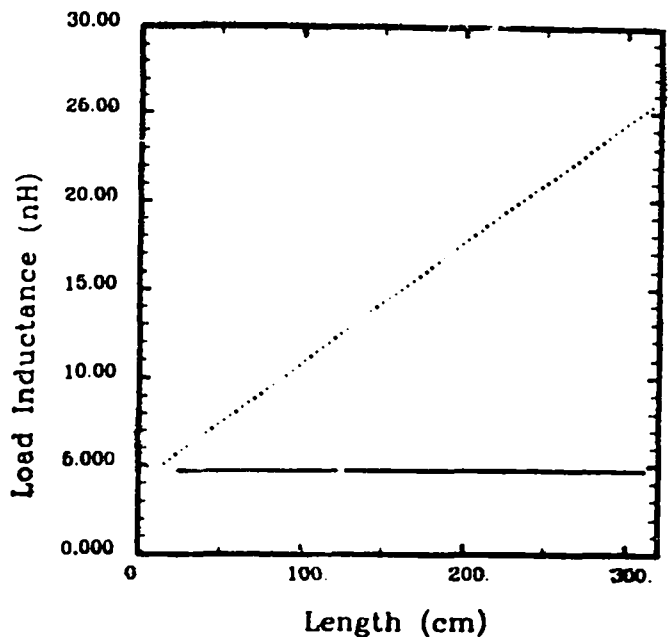


Fig. 5. Load inductance vs length for 30-cm-radius inside-out coax (solid) and disk (dotted) FCGs with $\Delta = 1$ cm. Wasted transmission line inductance is added to the load inductance for the disk. There is no wasted inductance for the coax.

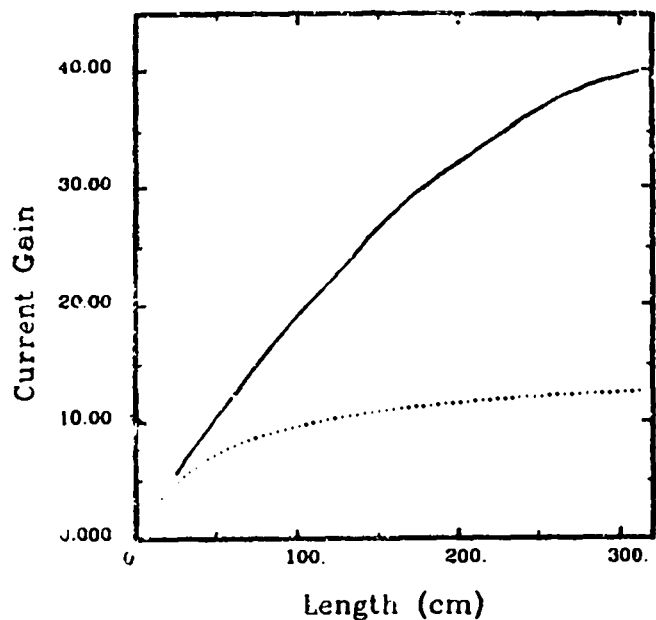


Fig. 6. Expected current gain vs length for 30-cm-radius inside-out coaxial (solid) and disk (dotted) FCGs with $\Delta = 1$ cm. A value of 70% flux conservation is used for the coaxial and 75% for the disk.

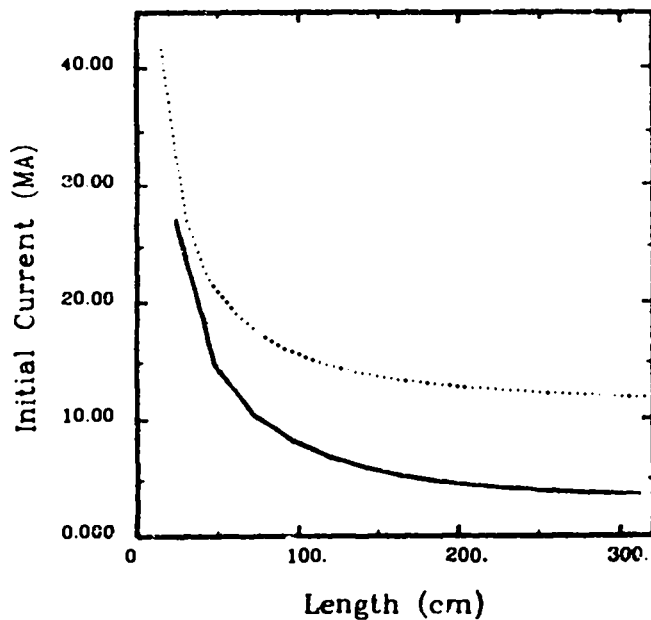


Fig. 7. Initial load current required to produce 150-MA final current vs length for 30-cm-radius inside-out coaxial (solid) and disk (dotted) FCGs with $\Delta = 1$ cm.

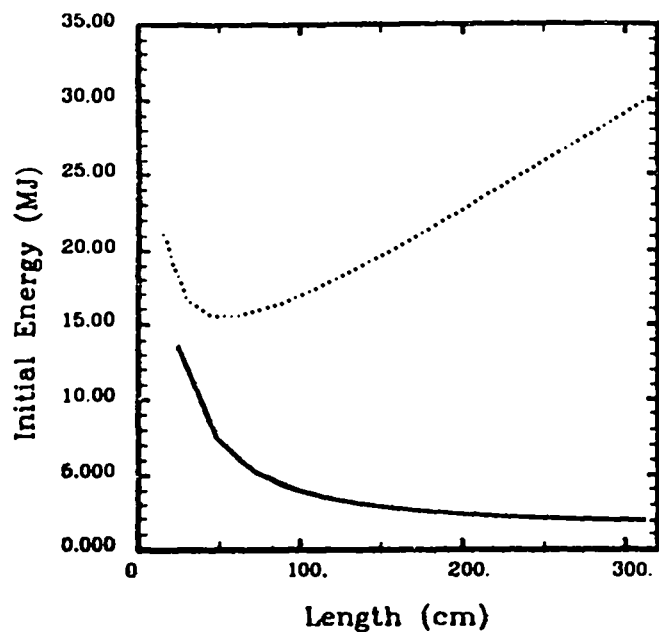


Fig. 8. Initial load energy required to produce 150-MA final current vs Length for 30-cm-radius inside-out coaxial (solid) and disk (dotted) FCGs with $\Delta = 1$ cm.

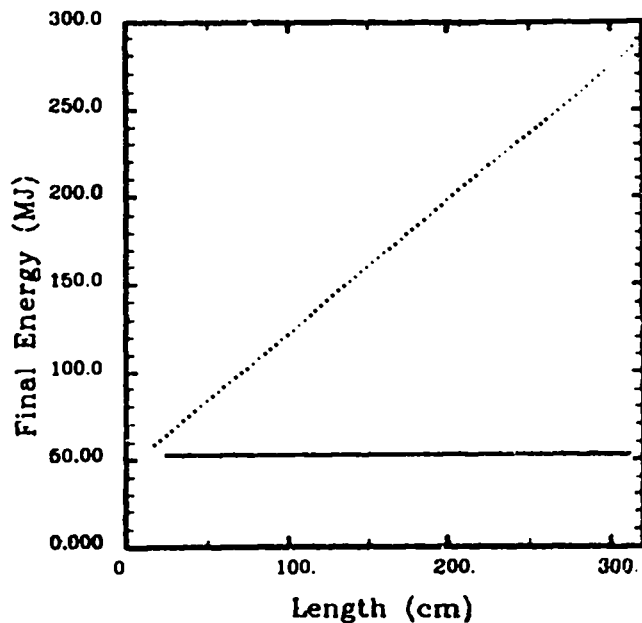


Fig. 9. Final load energy at 150 MA vs length for 30-cm-radius inside-out coaxial (solid) and disk (dotted) FCGs with $\Delta = 1$ cm. The disk must produce more energy because of its larger load inductance (Fig. 4); however, both generators produce the same peak field in the load.

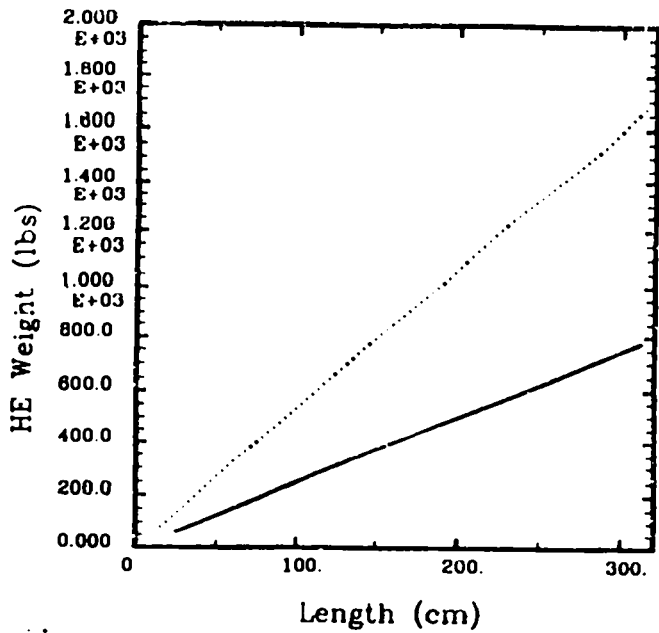


Fig. 10. HE weight vs Length for 30-cm-radius inside-out coaxial (solid) and disk (dotted) FCGs with $\Delta = 1$ cm.

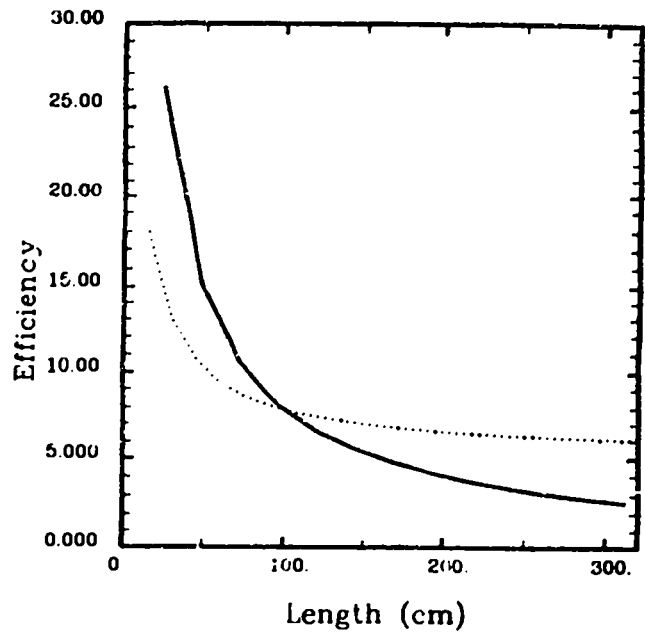


Fig. 11. Required efficiency vs length for 30-cm-radius inside-out coax (solid) and disk (dotted) FCGs with $\Delta = 1$ cm. Note that higher efficiency implies a more risky design relative to each type. Efficient robust designs have reported efficiencies on the order of $\leq 10\%$, though higher efficiencies have been reported.

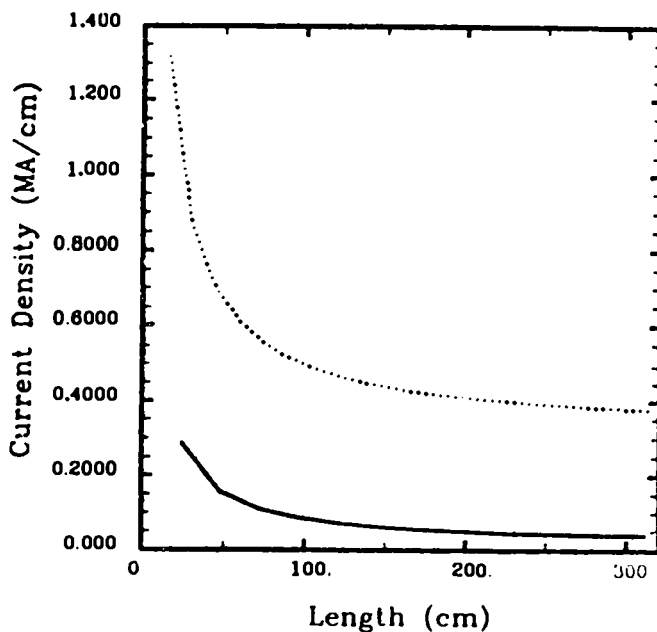


Fig. 12. Required linear current density sustained during initial loading to produce 150-MA output vs length for 30-cm-radius inside-out coaxial (solid) and disk (dotted) FCGs with $\Delta = 1$ cm.

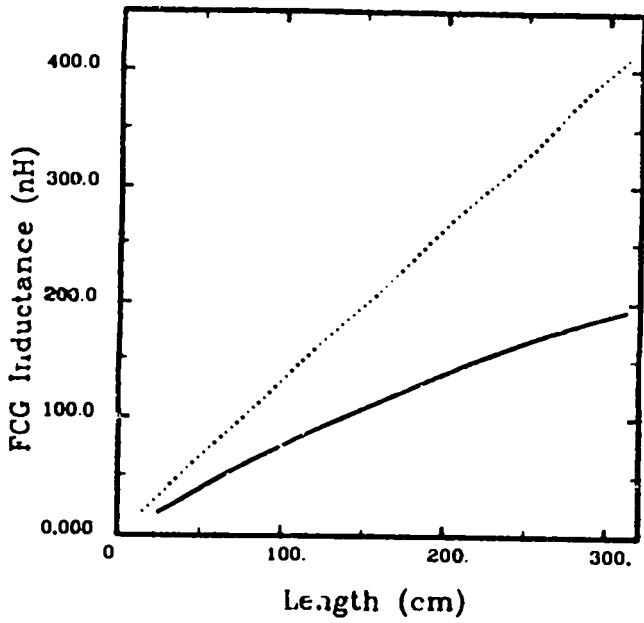


Fig. 13. Inductance vs length for 30-cm-radius inside-out coaxial (solid) and disk (dotted) FCGs with $\Delta = 0.5$ cm.

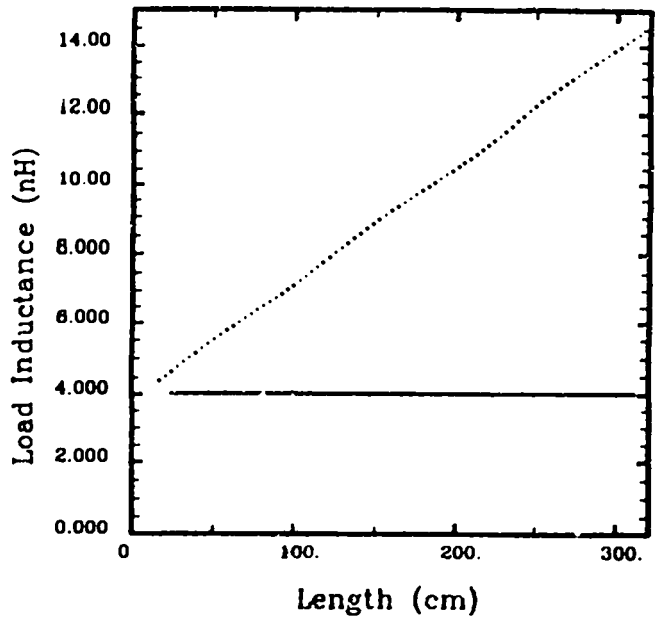


Fig. 14. Load inductance vs length for 30-cm-radius inside-out coax (solid) and disk (dotted) FCGs with $\Delta = 0.5$ cm. Wasted transmission line inductance is added to the load inductance for the disk. There is no wasted inductance for the coax.

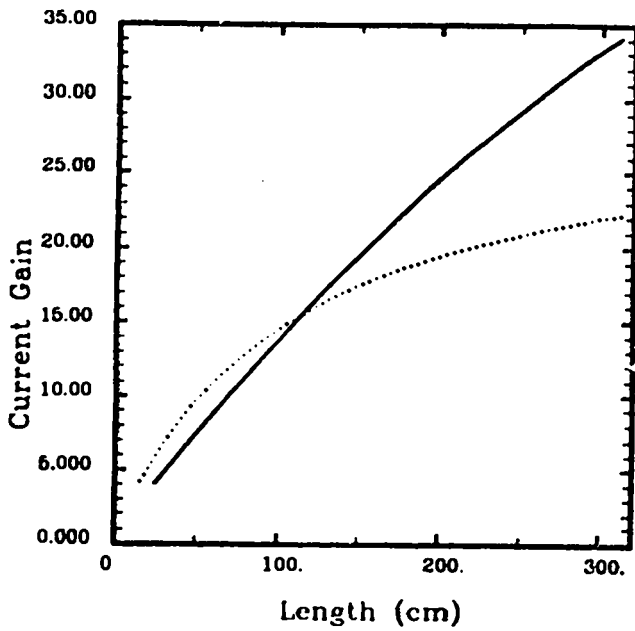


Fig. 15. Expected current gain vs length for 30-cm-radius inside-out coaxial (solid) and disk (dotted) FCGs with $\Delta = 0.5$ cm. A value of 70% flux conservation is used for the coaxial and 75% for the disk.

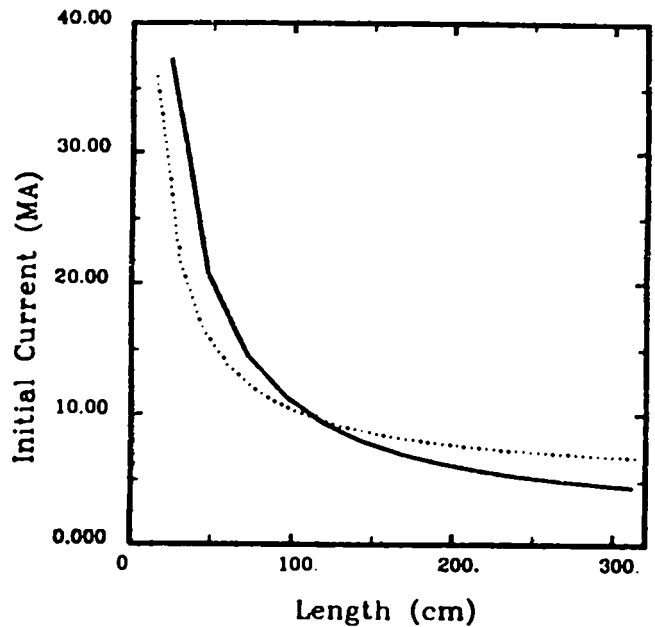


Fig. 16. Initial load current required to produce 150-MA final current vs length for 30-cm-radius inside-out coaxial (solid) and disk (dotted) FCGs with $\Delta = 0.5$ cm.

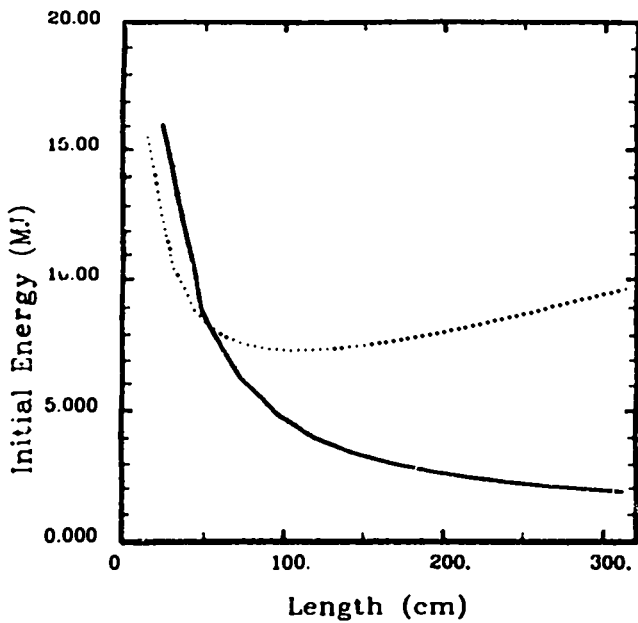


Fig. 17. Initial load energy required to produce 150-MA final current vs length for 30-cm-radius inside-out coaxial (solid) and disk (dotted) FCGs with $\Delta = 0.5$ cm.

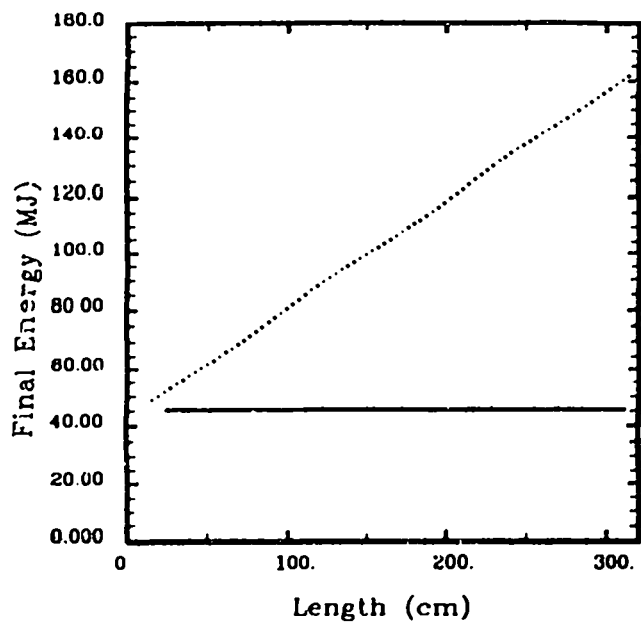


Fig. 18. Final load energy at 150 MA vs length for 30-cm-radius inside-out coaxial (solid) and disk (dotted) FCGs with $\Delta = 0.5$ cm. The disk must produce more energy because of its larger load inductance (Fig. 4); however, both generators produce the same peak field in the load.

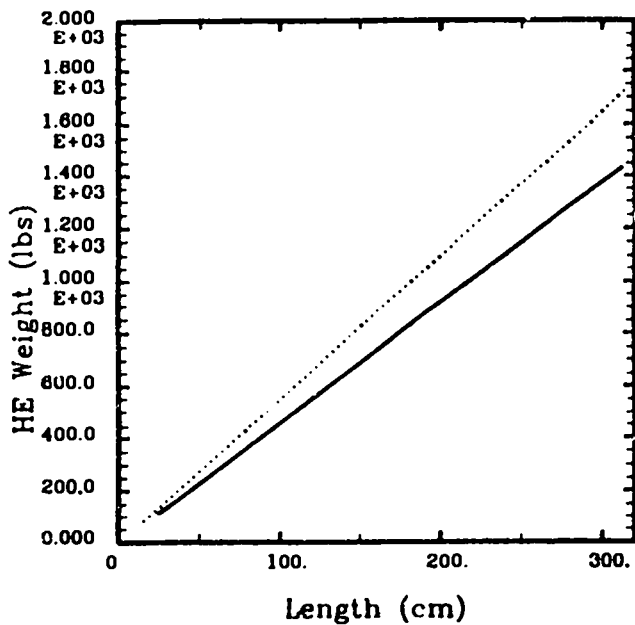


Fig. 19. HE weight vs length for 30-cm-radius inside-out coaxial (solid) and disk (dotted) FCGs with $\Delta = 0.5$ cm.

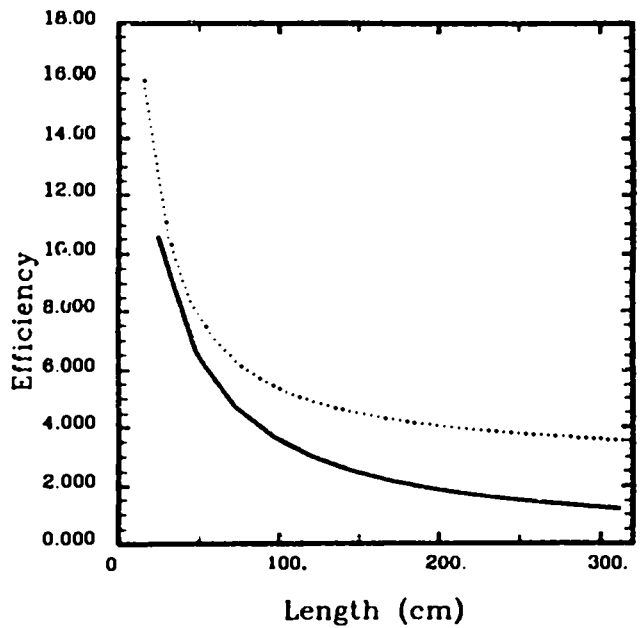


Fig. 20. Required efficiency vs length for 30-cm-radius inside-out coaxial (solid) and disk (dotted) FCGs with $\Delta = 0.5$ cm. Note that higher efficiency implies a more risky design relative to each type. Efficient robust designs have reported efficiencies on the order of 10%, though higher efficiencies have been reported.

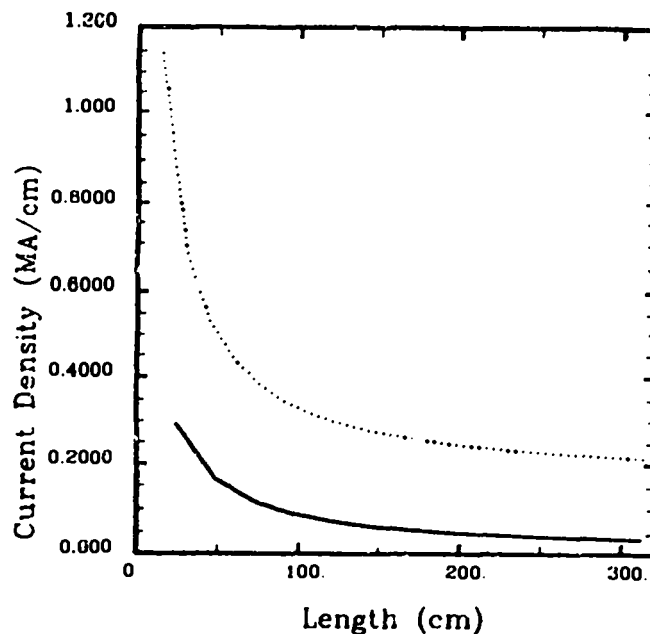


Fig. 21. Required linear current density sustained during initial loading to produce 150-MA output vs length for 30-cm-radius inside-out coaxial (solid) and disk (dotted) FCGs with $\Delta = 0.5$ cm.

VI. OUTSIDE-IN COAXIAL FCG'S

The generic outside-in coaxial FCG chosen for this study is shown in Fig. 3. Generator inductance is given by

$$L_g = \mu_o W_g [\ln(r_o/r_1) - r_2 \cdot \ln(r_1/r_2)/(r_1 - r_2) + 1]/(2\pi) \quad , \quad (21)$$

and load inductance has the form

$$L_l = \mu_o w \cdot \ln(r_2/r_1)/(2\pi) \quad , \quad (22)$$

where the load width, w , is assumed to be 1 cm as before. Notice that no standoff distance is required for load protection, and there is no obvious wasted inductance. Setting $r_2 = r_1$ gives zero load inductance and implies that an infinite current gain would be possible if the load were static and the simple assumptions used in the two previous sections could be applied. The flaw in the argument is associated with linear current densities approaching 5 MA/cm for 150 MA at a 5-cm radius. Overlooking this problem temporarily, two additional obstacles associated with the outside-in design are the large mass of HE and the very large area initiation system needed to set up the simultaneous detonation wave. These two problems are technologically tractable, given sufficient capital and time. Furthermore, if the linear current density show-stopper could be conquered, the required development costs would be a bargain.

To investigate the severity of the current density limit, RAVEN calculations of an outside-in coaxial FCG of 200 nH driving a 0-nH load were run in a quasi-2D mode. The calculations involved ten 1D-MHD modules coupled through the sophisticated circuit package in RAVEN. Analogous calculations were run for the CN-III inside-out experiments and agreed very well with the data.⁸

Generator parameters for this calculation were chosen to be as close as possible to an inside-out CN-III turned outside-in. The parameters, illustrated in Fig. 3, were chosen as follows: $W_g = 144.12$ cm, $r_l = 5$ cm, $r_2 = 5$ cm, $r_1 = 11.29$, $\theta = 2.5^\circ$, and $r_o = 15.88$ cm. The initial current was 3.2 MA loaded from a circuit that represents all four modules of the Firing Point 88 capacitor bank charged to 18 kV. Figure 31 gives the calculated current profile produced in the zero-inductance short circuit load. The peak current was 105 MA, which represents a whopping 3.3 MA/cm at a radius of 5 cm. Material interface positions for the MHD module closest to the load are shown in Fig. 32 as a function of time. The armature and stator surfaces do make contact, wiping out the vacuum field region. However, as the current exceeded 55 MA at 82 μ s in this calculation (1.7 MA/cm or 2.2 MG at 5 cm), magnetic flux began penetrating into the armature and stator very rapidly. Both the armature and stator surfaces were vaporized by the associated resistive heating. A careful look at the armature density and field profiles indicates that the vaporized surface layer allowed field to stream through while the remaining higher density portion of the armature, and hence more conductive portion, was stopped by the magnetic back pressure. This process, which traps magnetic flux in a stagnated armature, prevents further current amplification. Significant magnetic flux is also lost into the vaporized surface layer of the stator. Velocity profiles of the armature and stator interfaces are shown in Fig. 33. The vaporization of the surfaces is evident at 82 μ s.

Sensitivity studies for the outside-in coaxial were also run on RAVEN. Zoning of the armature and stator interfaces, equations of state, and electrical resistivity models were varied. The actual onset of vaporization was mildly sensitive to these changes. Nevertheless, the limiting current of ~ 100 MA was not sensitive to any of these variations. If a particular equation of state, zoning, and resistivity model delayed vaporization in a calculation, the magnetic back pressure effectively slowed the armature surface rather than slowing the armature interior. The end result in all of the calculations was that magnetic field energy prevents complete flux compression and/or is dissipated by resistive heating to limit the final current of an outside-in coaxial FCG, with a stator radius of 5 cm, to ~ 100 MA. Since this current is well below that required for this study, and the developmental costs associated with large HE charges and outside-in initiation systems are quite large, the outside-in coaxial FCG is not suitable for this application.

VII. LOWER CURRENTS AND HIGHER INDUCTANCES

For z-pinch applications with very small mass loads, lower currents are required. However, they must be delivered on a much faster timescale. For example, one advanced master concept calls for ~ 50 MA to be delivered to a ~ 20 -nH load, which includes an opening switch. This switch serves the purpose of pulse compression from the generator timescale, including the initial loading time, to the microsecond implosion timescale.

For purposes of comparison, it is assumed that a 20-cm-radius FCG is sufficient to generate 50 MA into 20 nH. A family of inside-out coaxial FCGs with $r_o = 10$ cm, $r_i = 20$ cm, and $\theta = 1^\circ$ (see Fig. 1) is compared, in Figs. 34–38, to a family of disk FCGs with a , b , c , d , e , f , x , y , z , and t equal to 4, 8, 8, 19, 19.75, 20, 3.27, 0.5, 5, and 0.5 cm, respectively (see Fig. 2). A 0.25-cm transmission line was chosen to minimize wasted inductance. Since internal voltages should be less in this application, this narrow transmission line may be possible if HE shocks and magnetically induced motion in the generator can be controlled. Each disk module has a width $W = 11.55$ cm and an inductance $L_g = 11.31$ nH. Waste transmission line inductance, L_t , is held to 0.29 nH per module. Operating times for the coaxial and the disk are 43.48 and 19.22 μ s, respectively. Therefore, either type must employ an opening switch to protect the load. Figure 34 shows FCG inductance versus length for the two families of generators. Notice that the disk lies below the coaxial out to 300 cm and beyond. Making the armature radius, r_o , larger for the coaxial FCG would lower both the generator inductance and the operating time. On the other hand, much could be gained by decreasing the values of a and b for the disk, which would increase module inductance significantly while only increasing operating times slightly. Unfortunately, as a and b are decreased, magnetically induced motion during the loading phase becomes more of a problem because of higher linear current densities. Load inductances for the disk and the coaxial FCGs are shown in Fig. 35, where the wasted transmission line inductance is included in the load inductance for the disk as before. Expected current gain is shown in Fig. 36. Notice the lower gains for both types of generators because of the higher load inductances. Gains of less than five represent unacceptable performance, which implies that either type of FCG will have to be at least 150-cm long. Required initial currents are shown in Fig. 37. By combining the data in Figs. 36 and 37, one can verify that the peak output current will be 50 MA, i.e., working backwards in the model reproduces the input parameters. Figure 38 shows initial loading energies for both FCGs, and indicates that the disk requires both a larger energy and input current to produce the same peak output current.

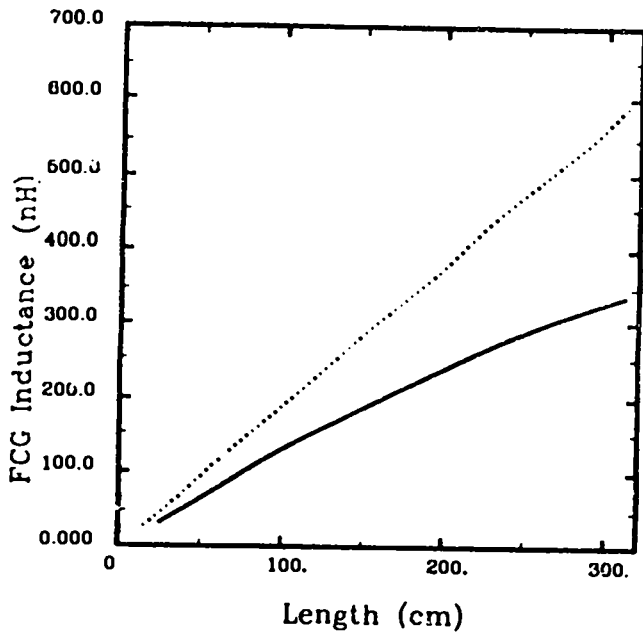


Fig. 22. Inductance vs length for 50-cm-radius inside-out coaxial (solid) and disk (dotted) FCGs with $\Delta = 1$ cm.

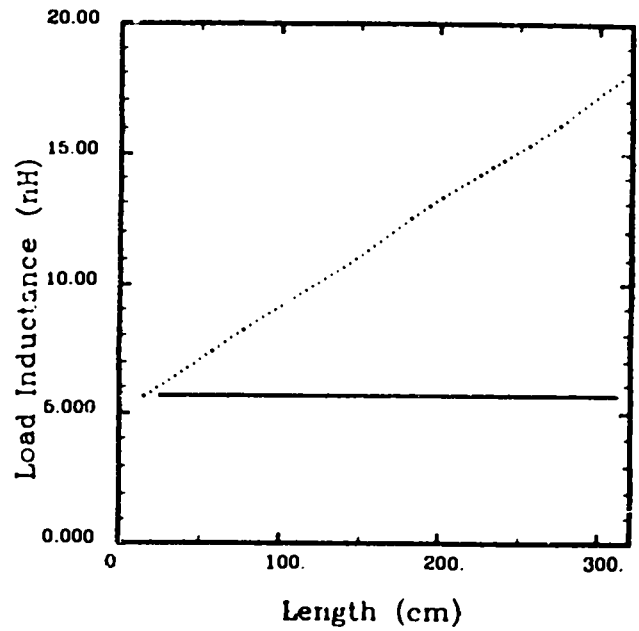


Fig. 23. Load inductance vs length for 50-cm-radius inside-out coax (solid) and disk (dotted) FCGs with $\delta = 1$ cm. Wasted transmission line inductance is added to the load inductance for the disk. There is no wasted inductance for the coax.

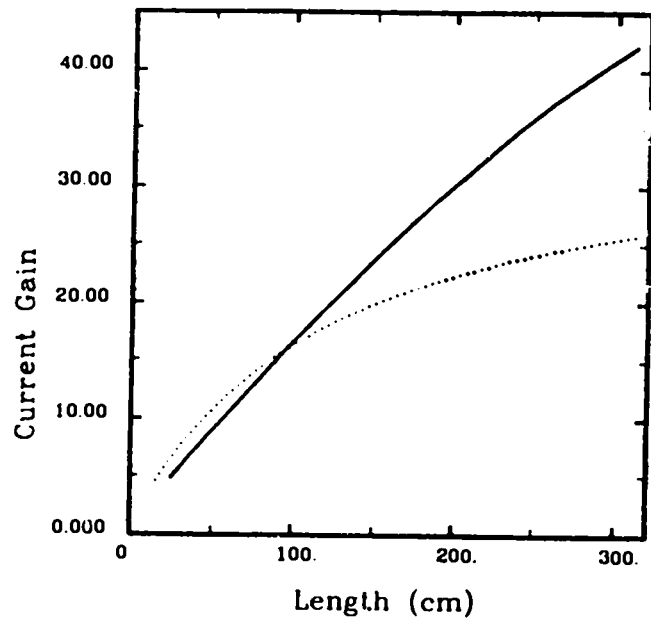


Fig. 24. Expected current gain vs length for 50-cm-radius inside-out coaxial (solid) and disk (dotted) FCGs with $\delta = 1$ cm. A value of 70% flux conservation is used for the coaxial and 75% for the disk.

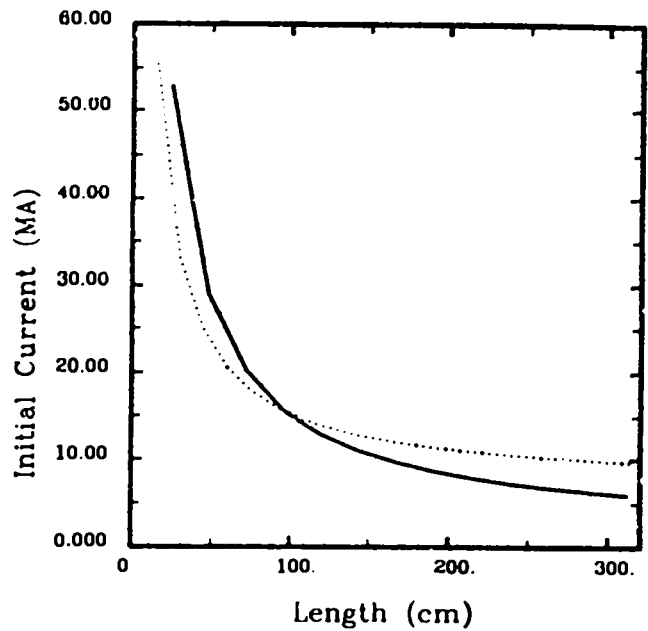


Fig. 25. Initial load current required to produce 250-MA final current vs length for 50-cm-radius inside-out coaxial (solid) and disk (dotted) FCGs with $\delta = 1$ cm.

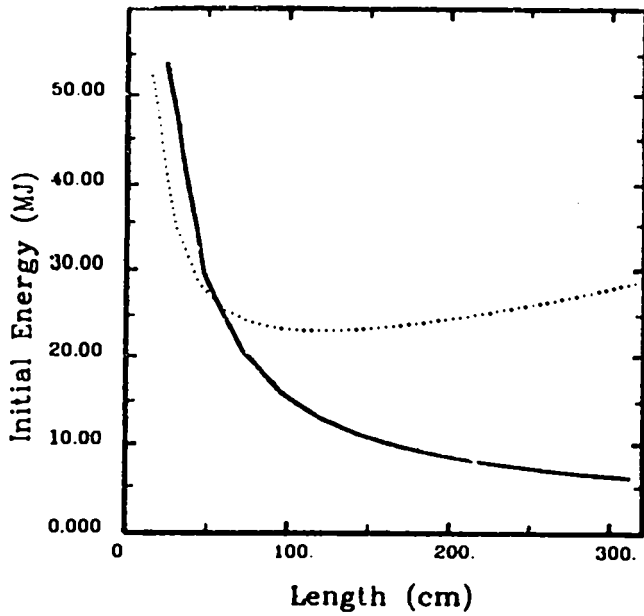


Fig. 26. Initial load energy required to produce 250-MA final current vs length for 50-cm-radius inside-out coaxial (solid) and disk (dotted) FCGs with $\delta = 1$ cm.

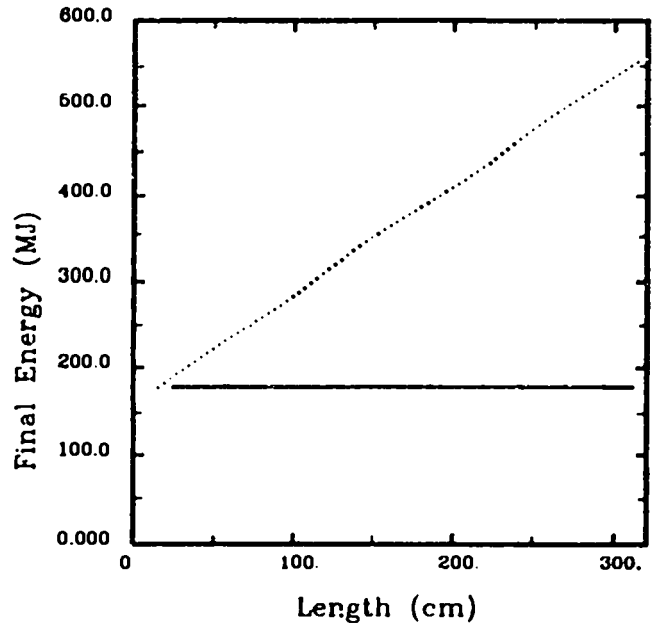


Fig. 27. Final load energy at 250 MA vs length for 50-cm-radius inside-out coaxial (solid) and disk (dotted) FCGs with $\delta = 1$ cm. The disk must produce more energy because of its larger load inductance (Fig. 4); however, both generators produce the same peak field in the load.

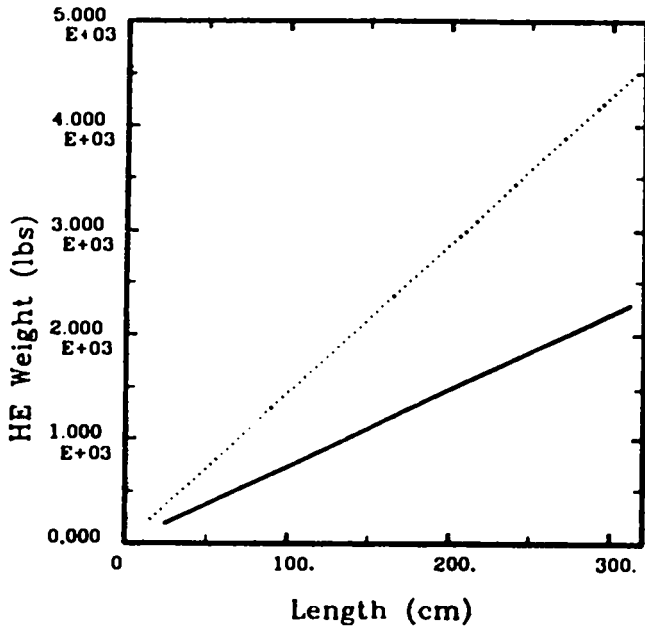


Fig. 28. HE weight vs length for 50-cm-radius inside-out coaxial (solid) and disk (dotted) FCGs with $\delta = 1$ cm.

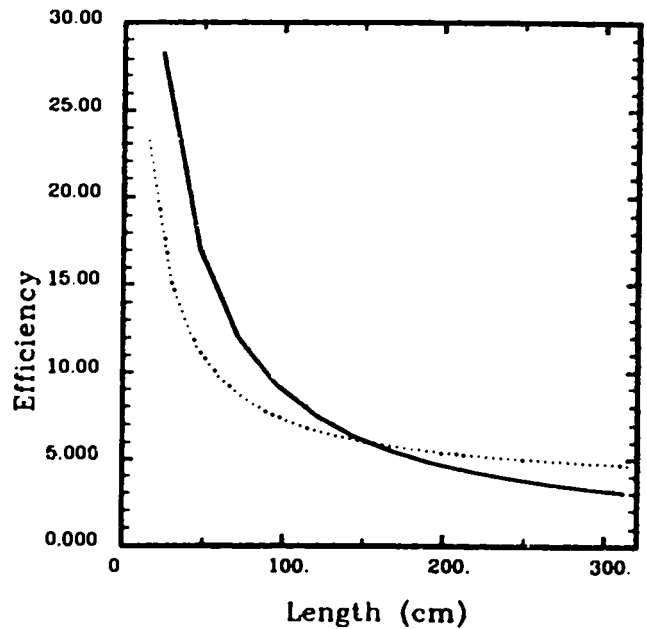


Fig. 29. Required efficiency vs length for 50-cm-radius inside-out coax (solid) and disk (dotted) FCGs with $\delta = 1$ cm. Note that higher efficiency implies a more risky design relative to each type. Efficient robust designs have reported efficiencies on the order of $\leq 10\%$, though higher efficiencies have been reported.

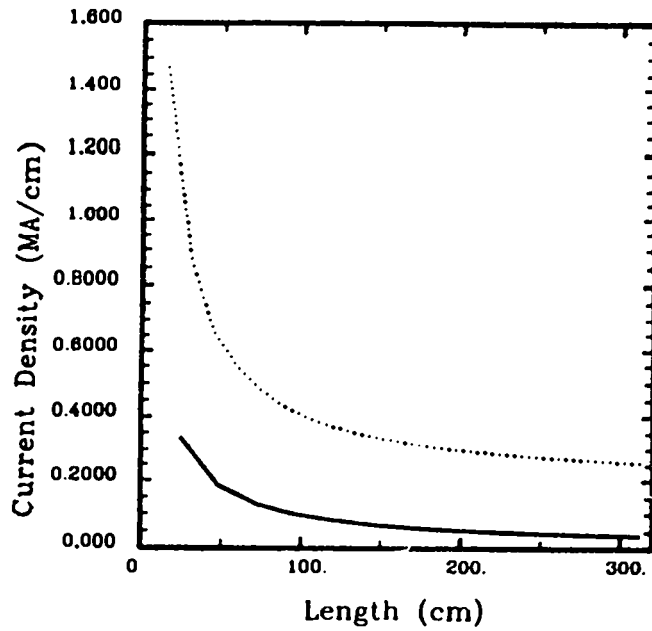


Fig. 30. Required linear current density sustained during initial loading to produce 250-MA output vs length for 50-cm-radius inside-out coaxial (solid) and disk (dotted) FCGs with $\delta = 1$ cm.

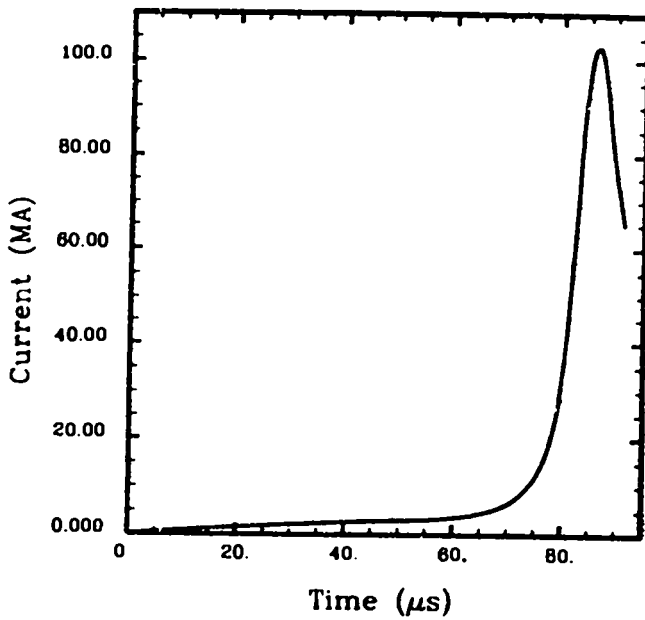


Fig. 31. Current profile for outside-in coaxial FCG from RAVEN.

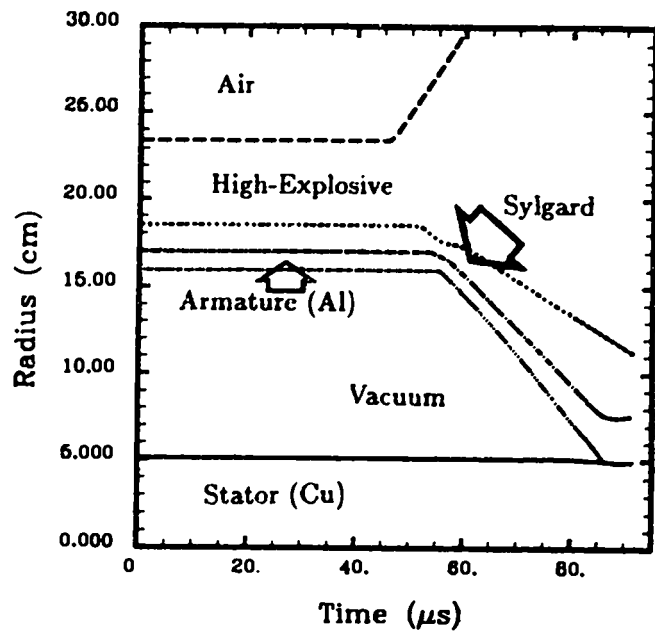


Fig. 32. Interface position vs time for outside-in coaxial FCG from RAVEN.

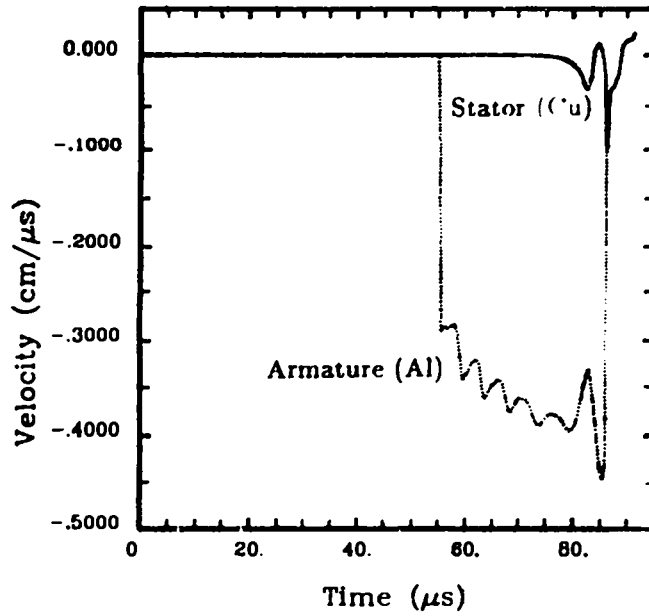


Fig. 33. Armature and stator velocity for outside-in coaxial FCG from RAVEN.

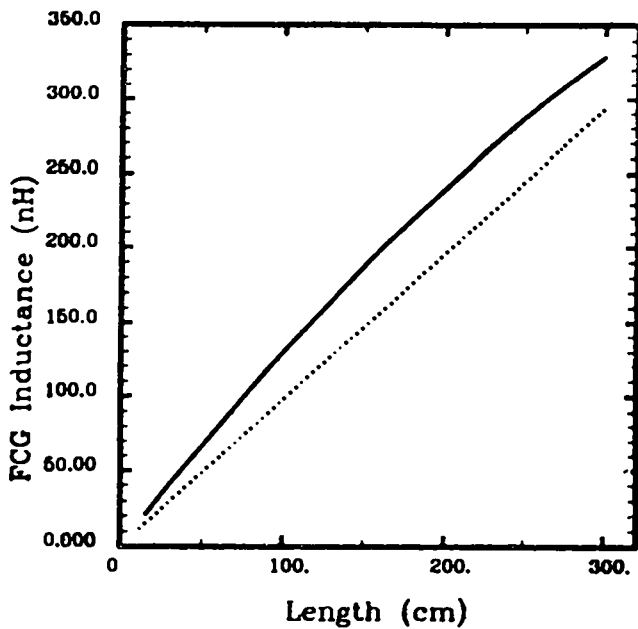


Fig. 34. Inductance vs length for 20-cm-radius inside-out coaxial (solid) and disk (dotted) FCGs with 20-nH external load and 50-MA peak current.

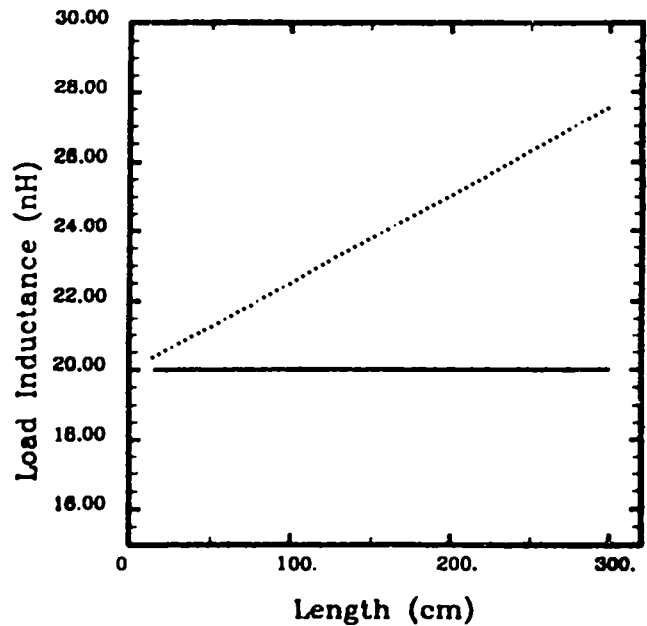


Fig. 35. Load inductance vs length for 20-cm-radius inside-out coax (solid) and disk (dotted) FCGs with 20-nH external load and 50-MA peak current. Wasted transmission line inductance is added to the load inductance for the disk. There is no wasted inductance for the coax.

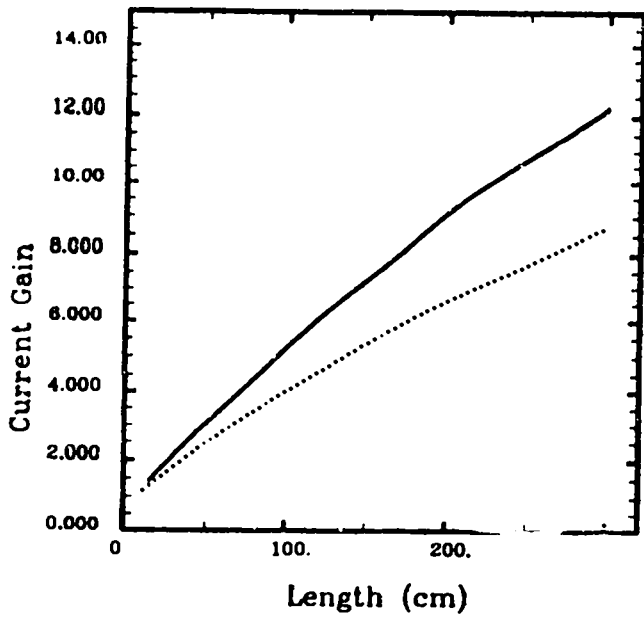


Fig. 36. Expected current gain vs length for 20-cm-radius inside-out coaxial (solid) and disk (dotted) FCGs with 20-nH external load and 50-MA peak current. A value of 70% flux conservation is used for the coax and 75% for the disk.

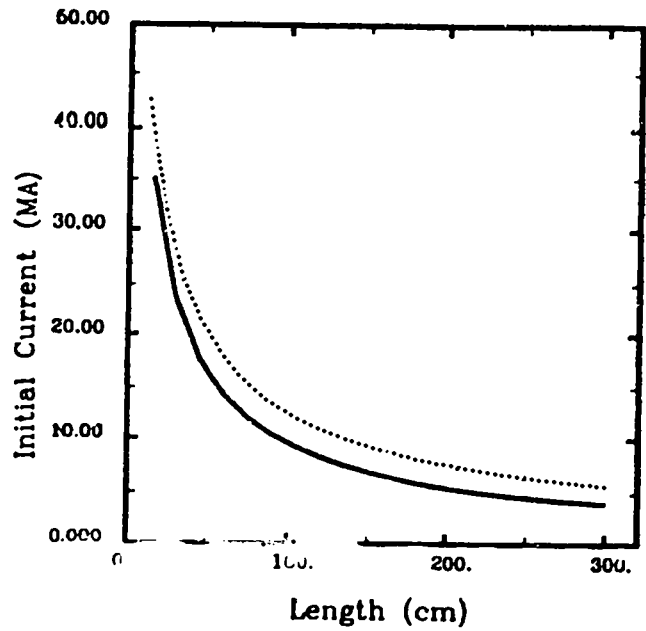


Fig. 37. Initial load current vs length for 20-cm-radius inside-out coax (solid) and disk (dotted) FCGs with 20-nH external load and 50-MA peak current.

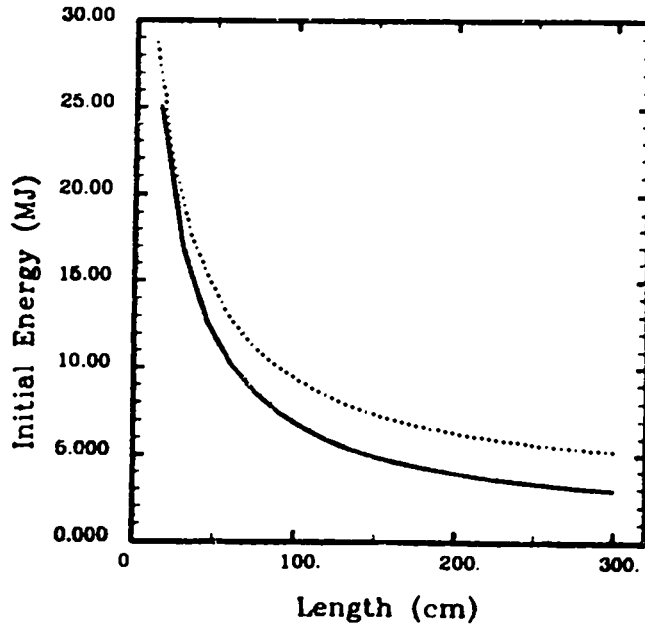


Fig. 38. Initial load energy vs length for 20-cm-radius inside-out coax (solid) and disk (dotted) FCGs with 20-nH external load and 50-MA peak current.

VIII. SUMMARY

For the high-current application, the inside-out coaxial design is quite attractive. It is capable of doing the job with a simple geometry design and existing components that have been proven. The CN-III experiments have quantified the conclusions drawn in this report concerning the inside-out coaxial FCG.

Disk FCGs are also capable of generating the required currents as reported in the Russian papers.^{1,2-7} However, they are more complicated, require larger input currents and energies, require more HE, and waste a significant fraction of their energy in transmission line inductance. Disk FCGs are faster than coaxial systems but by less than a factor of two. Simultaneous coaxial FCGs make up for some of this lack of speed by having a faster rising pulse near burnout than the disks have, relative to their respective operating times. For systems that use switching to protect the load from the initial phase of flux compression, the final e-folding time of the FCG current waveform becomes more important than the total operating time.

In regard to the outside-in coaxial FCGs, even if total HE mass and large area initiation were not a problem, outside-in designs are not capable of generating the peak currents required. It is suggested that these FCGs not be pursued in this context.

In the Trailmaster application, the choice of generator is not definitive. Other comparisons between disks and coaxial FCGs are possible, and since the performance difference is smaller for this application, either type of generator could probably be employed. The primary supporting issue for the disk is its faster operating time, which lessens the strain on opening switch design. However, the negative aspects should be weighed thoughtfully before incorporating these generators into the design of an experimental program. They include lack of experience with disk FCGs in this country, difficult and tricky transmission line design, complicated HE and conductor shapes, assembly difficulties, and larger HE charges. The coaxial FCG design, on the other hand, is much closer to being "off the shelf" and has a high probability of success. It is simpler to build and therefore probably more robust and repeatable. Nevertheless, if adequate resources were available, it would be desirable to test some of the disk generators.

ACKNOWLEDGMENTS

Many fruitful discussions with C. M. Fowler during the design and fielding stages of the CN-III experiments have helped to shape the authors' understanding of high-performance FCGs. The authors also acknowledge helpful discussions with R. E. Reinovsky and I. R. Lindermuth concerning Russian designs presented at Megagauss V. Finally, T. Oliphant's code development in RAVEN, specifically for the quasi-2D CN-III calculations, provided a new capability and is very much appreciated.

REFERENCES

1. A. I. Pavlovskii, R. Z. Lyudaev, B. A. Boyko, A. S. Boriskin, A. S. Kravchenko, V. E. Gurin, and V. I. Mamyshev, "Investigation of Disk Magnetocumulative Generators," in *Megagauss Fields and Pulsed Power Systems*, V. M. Titov and G. A. Shvetsov, Eds. (Nova Science Publishers, New York, 1989), pp. 331-336.
2. C. M. Fowler and R. S. Caird, "The Mark IX Generator," in *7th IEEE Pulsed Power Conference*, B. H. Bernstein and J. P. Shannon, Eds., pp. 475-478 (1989).
3. A. I. Pavlovskii, R. Z. Lyudaev, and B. A. Boyko, "Disk Magnetic Cumulation Generators Maximum Characteristics," in *Megagauss Field and Pulsed Power Systems*, V. M. Titov and G. A. Shvetsov, Eds. (Nova Science Publishers, New York, 1989), pp. 327-330.
4. V. K. Chernyshev, B. E. Grinevich, V. U. Vahrushev, and V. I. Mamyshev, "Scaling Image of ~90-MJ Disk Explosive Magnetic Generators," in *Megagauss Field and Pulsed Power Systems*, V. M. Titov and G. A. Shvetsov, Eds. (Nova Science Publishers, New York, 1989), pp. 347-350.
5. V. A. Demidov, A. I. Kraev, V. I. Mamyshev, A. A. Petrukhin, V. P. Pogorelov, V. K. Chernyshev, V. A. Shevtsov, and V. I. Shpagin, "Three-Module Disk Explosive Magnetic Generator," in *Megagauss Field and Pulsed Power Systems*, V. M. Titov and G. A. Shvetsov, Eds. (Nova Science Publishers, New York, 1989), pp. 351-354.
6. V. K. Chernyshev, M. S. Protasov, and V. A. Shvetsov, "The First Disk Explosive Generators," in *Ultrahigh Magnetic Fields: Physics. Techniques. Applications*, V. M. Titov and G. A. Shvetsov, Eds. (Moscow "NAUKA" 1984).
7. M. S. Protasov, B. V. Arkhipov, A. A. Petruhin, V. A. Prokopov, V. K. Chernyshev, and V. A. Shevtsov, "Fast-Acting Disk Explosive Magnetic Generator," in *Ultrahigh Magnetic Fields: Physics. Techniques. Applications*, V. M. Titov and G. A. Shvetsov, Eds. (Moscow "NAUKA" 1984).
8. B. L. Freeman, M. G. Sheppard, and C. M. Fowler, "Advanced High-Explosive Flux Compression Generator Development: The CN-III Series," LA report to be published.
9. T. A. Oliphant and K. H. Witte, "RAVEN," Los Alamos Report LA-10826, UC-32 (January 1987).
10. H. Knoepfel, *Pulsed High Magnetic Fields* (North Holland, Amsterdam, 1970); and "Very High Electromagnetic Energy Density Research at Frascati up to the Seventies and Beyond," in *Megagauss Technology and Pulsed Power Applications* C. M. Fowler, R. S. Caird, and D. J. Erickson, Eds. (Plenum Press, New York, 1987), pp. 7-18.
11. M. G. Sheppard, B. L. Freeman, R. L. Bowers, J. H. Brownell, C. M. Fowler, J. N. Fritz, A. E. Greene, S. P. Marsh, T. A. Oliphant, D. L. Tubbs, and D. L. Weiss, "Design, Testing, and Modeling of a High-Gain Magnetic Flux Compression Generator," in *Megagauss Technology and Pulsed Power Applications*, C. M. Fowler, R. S. Caird, and D. J. Erickson, Eds. (Plenum Press, New York, 1987), pp. 479-488.
12. C. M. Fowler, R. S. Caird, B. L. Freeman, and S. P. Marsh, "Design of the Mark 101 Magnetic Flux Compression Generator," in *Megagauss Technology and Pulsed Power Applications*, C. M. Fowler, R. S. Caird, and D. J. Erickson, Eds. (Plenum Press, New York, 1987), pp. 433-439.

13. B. L. Freeman, C. M. Fowler, J. C. King, A. R. Martinez, J. B. VanMarter, L. R. Veaser, and J. E. Vorthman, "Testing of the Mark 101 Magnetic Flux Compression Generator," in *Megagauss Technology and Pulsed Power Applications*, C. M. Fowler, R. S. Caird, and D. J. Erickson, Eds. (Plenum Press, New York, 1987), pp. 441-445.
14. Jacques Morin and J. Vedel, "Générateurs de Courants Intenses Par Conversion d'Énergie Explosives en Énergie Électrique," *C. R. Acad. Sci. Paris, T 272*, Ser. B, pp. 1-4 (1971).
15. E. I. Bichenkov, "Explosive Generators," *Sov. Phys. Doklady* **12**, pp. 567-569 (1967).